UNIVERSITY OF TWENTE.

Witteveen + Bos

Modelling the impact of positioning and pole height of a row of beach buildings on dune morphology

Nino L. Zuiderwijk

Thesis MSc Civil Engineering and Management

June 2023

Chair Graduation Committee:
prof. dr. K.M. Wijnberg

Supervisors:
ir. M.H.P. Jansen
dr. ir. P. Pourteimouri
dr. ir. G.H.P. Campmans

Faculty of Engineering Technology,
Civil Engineering and Management
University of Twente
P.O. Box 217
7500 AE Enschede
The Netherlands

Preface

This master thesis marks the end of my time as a Civil Engineering student at the University of Twente. In the past 5 months, I have performed this research on the influence of a row of beach buildings on dune morphology. Throughout my studies, my passion for water engineering and flood defense has grown. Together with my interest in nature-based solutions, I decided to choose this topic for my master thesis project at the company Witteveen+Bos. It has been a challenging journey in which I have learned much about aeolian sediment transport and the dynamics of coastal sand dunes. Besides, I improved my modeling skills and acquired knowledge on the use of OpenFOAM. I hope that this research will help in future decision-making on the design and placement of beach buildings at the beach-dune interface.

I would like to thank my supervisors for giving me the opportunity to perform this research and helping me with all the questions I had throughout the entire process. On the side of Witteveen+Bos: Maarten Jansen who has provided me with a lot of knowledge on the practical side of beach buildings and coastal sand dunes. It was very helpful and fun to visit the beach houses at Kijkduin and Egmond aan Zee together to get insights into patterns that form around beach buildings in the field. From the University of Twente I would like to thank Paran Pourteimouri, Geert Campmans and Kathelijne Wijnberg. Paran has helped me a lot during our frequent chats to set up my research well and helped me get along with the model. Together with Geert, you kept me motivated throughout my graduation period and made me proud of my research with your positive comments on my work. Kathelijne has helped me to make my research relevant and has helped me to improve my research.

At last, I would like to thank my girlfriend, family and friends who have helped me throughout this process since it did not always go according to plan. Their enthusiasm and encouragement inspired me to perform this research and finalize my master thesis with pride. I am sincerely grateful to my parents who have given me the opportunity to perform this research at the Witteveen+Bos office in Rotterdam with their continuous support and willingness to accommodate me for this period.

I hope you will enjoy reading my master thesis!

Nino Zuiderwijk

Enschede, June 2023

Summary

Beach buildings are often placed in rows in front of coastal sand dunes for recreational purposes. With the placement of a row of buildings, airflow-induced aeolian sediment transport is altered in the vicinity of the buildings. As a result, bed morphology over the dune profile and around the row of buildings may be altered. The influence of the row of buildings depends on various building characteristics. In specific, this thesis focuses on the influence of varying pole height and distance between the row of buildings and dune.

For the computation of change in bed morphology a model has been used that couples a 3D airflow model in OpenFOAM with a 2D-horizontal aeolian sediment transport model, AeoLiS. Simulations were conducted by modeling a row of beach buildings upwind of a vegetated coastal dune profile. The distance between the row of buildings and dune as well as the height of the poles were systematically varied throughout this study. A range of variations was examined, starting from zero (for buildings placed directly at the dune toe or on the bed) to greater distances and increased pole heights.

The bed level change around a row of buildings and over the dune profile was computed. Findings showed that a row of beach buildings on poles causes strong erosion around the buildings whereas deposition is enhanced over the dune toe. Although effects on the dune slope and top are minimal, our findings indicate a negative impact on dune growth over the dune slope and a positive effect over the dune top. Increasing pole height generally creates stronger sedimentation-erosion patterns in the vicinity of the buildings. The impact of the buildings on dune morphology decreases as the buildings are placed at larger distance from the dune. The sand supply in the dune is maximized when buildings are placed on long poles at substantial distance from the dune. However, this may result in strong longshore variation in bed level elevation if buildings are placed too close to the dune toe. In addition, results indicated that the critical gap width ratio as found in previous research, lowers for buildings on longer poles. The presence of vegetation over the dune profile efficiently traps sediment and significantly reduces erosion, mainly at the dune crest.

The model that was used in this study is able to capture morphodynamics over a dune profile including a row of beach buildings. However, validation showed that the computed morphological development over a single day is similar to the seasonal

bed evolution as observed in the field, indicating an overestimation of the rate of morphological change in the model. Nevertheless, the magnitude and patterns of the computed morphological bed evolution roughly agrees with field data and are similar to findings by previous researchers. Therefore, the knowledge gained through this study can help coastal managers to make decisions on the design and placement of beach buildings in front of coastal sand dunes.

Keywords: Dune morphological change, Bed morphology around a row of Beach Buildings, Aeolian Sediment Transport, Computation Fluid Dynamics, OpenFOAM, AeoLiS

Contents

List of Figures

1. Introduction

1.1 Context

Sandy beaches are considered to be invaluable ecosystems that provide important services to people living in coastal communities [8]. These beaches are appreciated for, amongst others, their recreational service and attractiveness. To maximize the recreational service of sandy beaches, humans have been modifying coastlines worldwide. An example of such modification is the placement of buildings at the beach-dune interface, see figure 1. In the Netherlands, beach houses can often be found at the beach-dune interface in a row directly next to each other and wind cannot pass underneath the building since the buildings are placed on the bed, see figure 1 b. Depending on the geometry, dimensions, placement and composition, beach buildings affect the wind field in the vicinity [9]. As a result, aeolian sediment transport and bed morphology may be altered in the surrounding of the building.

A large area along the Dutch coast is protected by sand dunes, which are a highly dynamic nature-based flood defense. The dunes form an important flood defense that prevent coastal regions from being flooded [10] [11]. Coastal sand dunes are subjected to wave attack which induces erosion, though are able to recover naturally by means of wind flow-driven sediment supply originating from the sandy beach. This sediment is actively being trapped by the vegetation on the dunes which allows dune growth [12]. Aeolian transport occurs if wind-induced bed shear stress on sediment particles exceeds a certain threshold value [4]. Due to the reliability of dunes on wind-driven sediment transport, the placement of buildings in the beach-dune interface could highly affect the natural growth and recovery process of these flood defenses. As a result, the dune morphology may be changed with either negative or positive effects on the flood protection level of the dune [13] [9] [14] [1].

Various building design parameters can influence the effects of a row of beach houses on coastal dune morphology. To be able to get better understanding of these influences on the dynamics of a coastal dune, it is essential to perform research. Studies have been performed that aimed to improve understanding of bed morphological change around beach buildings (e.g. [3] [15]). The placement of buildings on the bed limits sediment transport in duneward direction and causes sand particles to be trapped [9] [15] [16]. However, elevating buildings on poles, without closure of the gap, allows wind to continue underneath the buildings which could reduce blocking effects and potentially even enhance sediment transport in duneward di-

Figure 1: a. Beach buildings on the Zuiderstrand near Kijkduin, adopted from Pourteimouri et al. [1] and b. Beach buildings on the beach side of a coastal dune adopted from WOTY webpage on beach houses [2].

rection [13], depending on the downwind distance from the building [1]. Knowledge that is created through these studies improves our understanding of the influence of beach buildings on dune morphology. The insights can be used to create advise on the placement and design of beach houses such that the negative effects of a row of beach buildings on morphological dune development are minimized and sediment transport towards the dune can potentially be enhanced if placed and designed correctly, as indicated by Pourteimouri et al. [1] and Hobeika [14].

1.2 Problem definition

Various studies have investigated the wind flow and sediment transport patterns around buildings on a beach or over a dune profile. Experiments have been performed by Poppema [15] on the sedimentation patterns that occur around a scaled building on a beach. In addition, multiple aeolian transport studies have made use of Computational Fluid Dynamics (CFD) to compute the wind field over a dune profile and around buildings on a beach and/or associated aeolian sediment transport [14] [17] [3] [18] [16]. Research by Hobeika [14] and Stevers [17] investigated the influence of the placement and orientation of a row of buildings with respect to each other, to the wind incidence angle and distance from the dune toe on wind flow and sediment transport patterns using CFD. Pourteimouri et al. [3] [16] investigated the influence of various building and wind characteristics on airflow, sediment transport and bed evolution patterns around a single building and row of buildings on a sandy beach surface and on elevated poles. In addition, a study performed by Jonkheer [18] investigated wind flow and sediment transport patterns over a dune profile as well as the influence of vegetation.

Pourteimouri et al. [1] developed a model that couples the CFD model OpenFOAM with the process-based numerical aeolian sediment transport model AeoLiS [19]. Pourteimouri et al. [1] used this coupled model to investigate the pole height of a row of buildings placed on a flat sandy beach on morphological bed level change. The coupling of CFD with the AeoLiS model is able to deal with sediment supply lim-

itations of the coastal sandy beach, for example, due to the presence of vegetation.

However, no previous research has quantified the influence of a row of beach buildings on dune morphodynamics over different sections of a dune profile while considering spatially and temporarily varying sediment supply limitations. In addition, previous research has shown the potential to enhance sediment transport in duneward direction for a specific distance to the dune toe [14] and a specific pole height [1]. Though neither of these studies has researched the combined influence of pole height and building distance from the dune toe over a vegetated coastal sand dune.

1.3 Research Objective

The goal of this research is to quantify the influence of a row of beach buildings in front of a vegetated coastal sand dune on bed morphology over the beach and dune as well as how pole height and building-to-dune distance influence morphology. In addition, this research aims to provide guidance on decisions for pole height and building to dune distance for a row of beach buildings in front of a vegetated coastal sand dune based on sand supply into the dune.

1.3.1 Research Questions

For this research objective, two research questions have been made. The first research question of this study addresses the influence of the placement of a row of buildings in front of a vegetated coastal dune on sedimentation patterns that occur over the dune profile:

1. How does a row of beach buildings on poles at the beach-dune interface alter bed morphology over a vegetated coastal dune profile?

The second research question will focus on two parameters of the placement and design of the row of buildings at the beach-dune interface, which are pole height and distance between the building and the dune. These two parameters affect aeolian sediment transport and associated bed morphodynamics in the vicinity of the buildings. Appropriate consideration of these two parameters may maximize sedimentation over different parts of the dune in the presence of a row of buildings.

2. How do varying pole height and building-to-dune distance of a row of beach buildings at the beach-dune interface alter bed morphology over a vegetated coastal dune?

1.3.2 Research approach and scope

To answer the research questions as given in section 1.3.1, this research is performed using the coupled model as proposed by Pourteimouri et al. [1]. The use of a model allows to get insight into a system's response to various modifications within the system, in this study varying pole height and building-dune distance, in a relatively cost and time-efficient manner when set up appropriately. However, models do not capture the true behaviour of a system but provide an approximation of

reality. For that reason, model validation will be performed to get insight into the performance and weaknesses of a model. The validation process is further elaborated in section 3.2.

The coupled model [1] has shown the potential to simulate sediment transport around a row of buildings on the beach [1] making it potentially suitable for computation of morphological bed level change over a dune profile with a row of beach buildings located upwind. The airflow model, OpenFOAM, is a 3D model and is able to compute the wind field around complex objects, such as a row of cubic buildings. The altered AeoLiS model is a 2DH model which uses the wind field as computed by OpenFOAM to simulate sedimentation patterns over the bed. Due to the high computational cost of the model, simulations will be performed over a period of 1 day without considering vegetation growth. To initiate significant sediment transport within this rather short period of time, a storm event is simulated.

1.4 Report outline

Chapter 2 provides an overview of relevant previous studies that have been performed. In chapter 3 the methodology which is used in this research is elaborately presented. Afterwards, the results are presented in chapter 4. These results are discussed extensively in chapter 5. At last, the conclusions of this research are presented in combination with the recommendations for further research in chapter 6.

2. Theoretical background

This chapter aims to investigate wind flow, sediment transport and associated morphological bed evolution in the vicinity of buildings on the beach in front of a vegetated coastal dune profile. The wind field over the bed is the driver for aeolian sediment transport. The associated entrainment and deposition of sediment alters the bed morphology. These changes, in turn, affect the wind field nearby, leading to a continuous feedback loop between the bed and wind field.

The feedback loop gives rise to highly dynamic bedforms, such as dunes. With the placement of buildings, static objects are added to the dynamic environment, continuously changing the dynamics of the bed. The changes to the bed form can either mitigate or enhance the effects of the buildings due to the interaction between the bed and wind field (e.g. burial or scour). In figure 2 a visualization of the feedback loop is given, containing a dynamic bed morphology and a static object, like a building. This chapter will discover the research that is performed on airflow, aeolian sediment transport and morphodynamics in the vicinity of buildings and dune profiles.

2.1 Air flow

Wind continuously flows around us with a certain direction and magnitude. The flow interacts and exerts stresses on surfaces over which it flows as well as on particles that are present at that surface. If the stresses on particles exceed a certain threshold, the particles are set to motion [4]. As a result, aeolian sediment transport happens and bed level change is initiated.

Airflow can become very chaotic and complex, making it difficult to compute a wind field for a specific case, which is of great importance for the computation of aeolian sediment transport. Various researchers have attempted to investigate and propose models that describe and compute airflow patterns at sandy beaches for the approximation of aeolian sediment transport at coastal environments [20] [13] [21] [22]. Generally, aeolian transport is induced by turbulent wind fields [4]. A turbulent flow contains fluctuations in wind speed over a wide range of spatial and temporal scales [4]. Shear stress on particles is a result of net vertical momentum flux of upper air layers onto the particles [23]. This shear stress can be approximated using an equation as has been used by Walker and Nickling [21]:

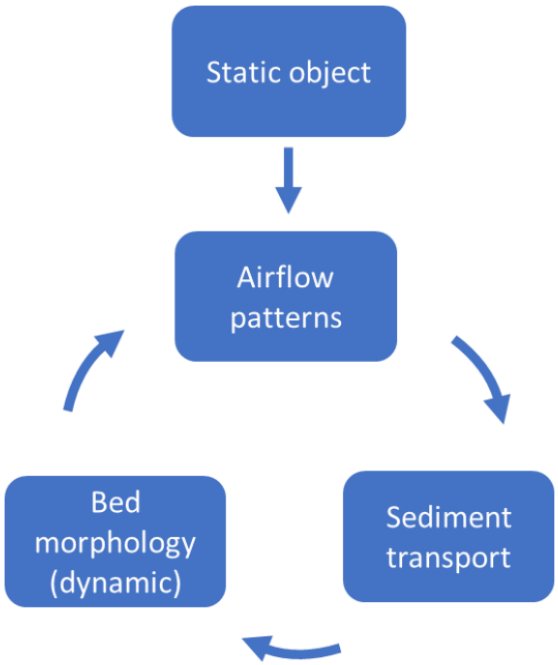

Figure 2: Morphological bed evolution loop that shows the interactions between relevant aspects adopted and modified from Pourteimouri et al. [3]

$$\tau = \rho u_*^2 \tag{1}$$

Where τ is the bed shear stress $[N/m^2]$ and ρ is the density of air $[kg/m^3]$. In addition, bed shear stress cannot be measured directly and thus is expressed by means of an additional parameter, u_*, the shear velocity $[m/s]$. The shear velocity at the lower wind speed profile of an incompressible and steady flow over a homogeneous surface can be computed using the logarithmic Prandtl-Von Kármán equation:

$$\frac{u_z}{u_*} = \frac{1}{\kappa} ln(\frac{z}{z_0}) \tag{2}$$

Where z is the height at which the horizontal velocity is measured in [m], u_z in [m/s] is the horizontal velocity at height z, κ is the dimensionless Von Kármán constant (≈ 0.4 [-]) and z_0 is a measure for the hydrodynamic roughness in [m].

Though at coastal environments with the presence of dune profiles, wind flow generically is non-logarithmic and unsteady, which highly affects the aeolian sediment transport over the dune profile [24]. Models have been created that tried to compute the wind field over a coastal dune profile [25] [26]. Though, these models are generally not valid due to the presence of jet flows or flow separation and can only be used to compute wind over a gentle windward slope [27]. Besides, over the past recent years, computational power has increased and as a result, aeolian sediment trans-

port studies have increasingly shifted to the use of Computational Fluid Dynamics (CFD). Therefore, the wind field in this thesis is computed using CFD.

Computational Fluid Dynamics is generally used in aeolian sediment transport to compute the complexity of the near-bed wind field in the boundary layer. CFD uses the Navier-Stokes equations to compute the wind field numerically over a meshed computational domain of a fluid flow [27]. The Navier-Stokes equations describe the flow of fluids and comprise the conservation of mass, momentum and energy. Due to the presence of non-linearity in airflow caused by turbulence, the solution to the Navier-Stokes equations becomes highly complex. For that reason, the solution to the Navier-Stokes equations is generally approximated by either Reynolds-Averaged Navier-Stokes (RANS) or Large Eddy Simulation (LES) which differ in the computation of turbulence. LES has the ability to maintain a physical measure of turbulence whereas RANS computes the wind field as mean and fluctuating components, reducing computation cost significantly compared to LES. Another method is Direct Numerical Simulation (DNS), though DNS requires an extreme amount of computation power, making it disfavored over the use of both RANS and LES. To close the set of equations, the k-ϵ is commonly applied which is a two-equation turbulence closure model that computes turbulent kinetic energy (k) and energy dissipation (ϵ) [28]. The RANS k-ϵ is commonly used for the simulation of airflow over aeolian landforms (e.g. [29] [16]) and requires significantly less computational power compared to other methods. For that reason, the RANS k-ϵ is applied in this study to compute the wind field.

Even though CFD is able to compute the fluid flow using the Navier-Stokes equations, it still comes with high computation cost and is not able to capture the actual wind field as would occur in the field. However, there are various advantages of using CFD for the computation of the wind field [27]. For example, CFD allows to approximate the wind field for a detailed, complex and large geometry with high resolution and can be easily be altered to test a wide range of cases, which becomes more difficult for wind tunnel experiments and other numerical models. Besides, the edge wall effects are minimized since airflow can exit the domain, which is not possible for wind tunnel experiments. An additional advantage compared to other numerical methods is that CFD is able to compute flow separation zones that occur due to momentum loss and adverse flow direction at bedforms, such as dune profiles.

Various studies have been performed which aimed to better understand the influence of wind incidence angle and dune slope inclination on wind magnitude and wind direction over a dune profile which can then be related to aeolian sediment transport [30] [31] [32] [33]. In addition, the study by Jonkheer [18] investigated the use of a more natural smooth shape at the dune toe and dune crest to minimize flow separation at the dune toe and dune crest. Besides, the shape of a dune profile causes lower wind velocity upwind of the dune toe and wind acceleration at the dune

crest [34] [35] [14] [18].

In comparison to the gently sloped dune profiles, buildings introduce rather sharp edges that highly influence the wind field in the vicinity, creating complex shapes and form a horseshoe-like vortex system [9] [15]. Flow separation, recirculation and vortex shedding may form at the sides and downwind of the building, depending on the level of turbulence in the flow, relative wind incidence angle, downwind length and obstacle design characteristics [36] [37] [17] [14]. Two important design parameters are gap width between buildings that are placed in a row and the placement of buildings on poles above the bed. Pourteimouri et al. [16] indicated that for a certain gap width, wind velocity between the buildings may be increased. Besides, elevated buildings allow airflow underneath the building and increase in velocity for a certain pole height to building width ratio. The increase in velocity is caused by the funneling effect which constrains the jet flow between the buildings [1].

2.2 Sediment transport

Sand is transported if wind reaches sufficient velocity, which is often in the order of 10^0 [m/s] [4]. As described by equation 1 and 2, the wind that blows onto a particle causes shear stresses on that particle. The particle is set to motion if the shear stress exceeds the threshold value.

Strong wind, in the order of 10^1 [m/s], exerts large shear stresses on sand particles at the bed. This may cause small sand particles to transport in suspension. If sand particles are sufficiently large, gravitational forces increase and become influential, causing the particles to jump and transport in the form of saltation. Saltation particles that impact with the bed can set particles on the bed to motion if the impact is sufficiently strong. As a result of this impact, grains may transport in the form of reptation. Larger grains may transport with constant contact to the bed, which is known as bedload [4]. Figure 3 shows these different transport forms.

The model proposed by Bagnold [38] is a widely used empirical model and is based on wind tunnel experiments. The model assumes a proportional relationship between sediment transport rate (q [kg/m/s]) and shear velocity (u_* [m/s]), if the shear velocity exceeds a threshold value (u_{*t} [m/s]) based on particle composition [38] [39]:

$$q = C_B(\frac{\rho}{g})u_*^3(\frac{d}{D})^{1/2} \tag{3}$$

$$\text{when } u_* > u_{*t} = A\sqrt{gd(\frac{\rho_s - \rho}{\rho})}$$

Where C_B is the empirical Bagnold coefficient [-], ρ is the fluid density [kg/m^3], g is the gravitational acceleration [m/s^2], d is the median grain size [m], D is the reference grain size [m], A is a parameter being either 0.1 (motion by fluid force only) or 0.085 (motion by the momentum of impacting grains during saltation) [-] and ρ_s is

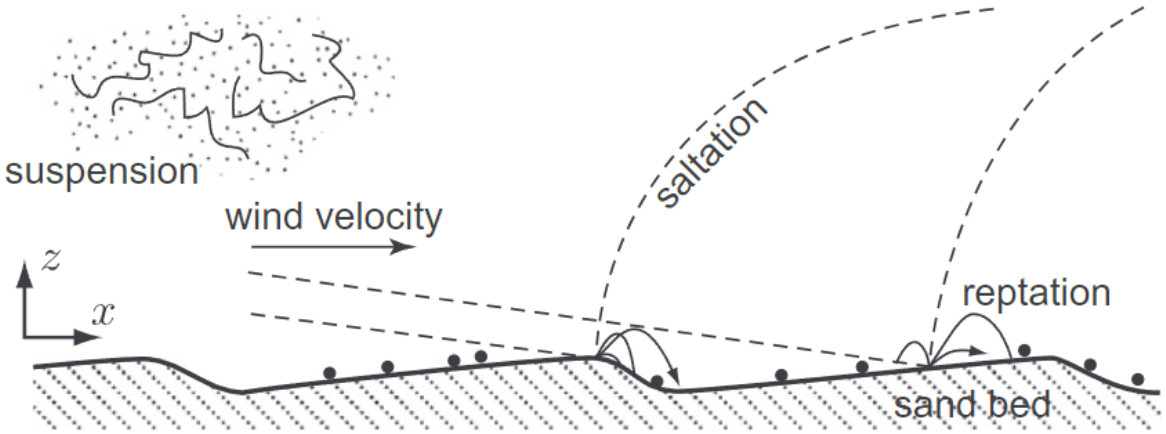

Figure 3: Schemetic overview of sediment transport modes adopted from Durán et al. [4].

the sediment density [kg/m^3].

Multiple models have been proposed that are additions to the model by Bagnold and are based on a similar relation (e.g. [40] [41] [42] [43] [44]). However, these models as well as the model by Bagnold itself are generally considered to overestimate aeolian sediment transport since these are based on wind tunnel experiments that do not incorporate the various sediment transport limiting factors that are present at the coastal sandy beach [23]. These limiting factors include amongst others vegetation, moisture content, beach armoring and fetch length. The sediment transport limiting factors cause bed surface properties and, as a result, sediment supply to differ spatially. Vegetation is commonly present on coastal sand dunes (see figure 1 b.). The presence of vegetation affects the bed surface properties in the vicinity. Vegetation mainly reduces bed shear stress, resulting in a reduction of sediment transport over the vegetation [12].

Recently two models have been created that include sediment supply limiting processes. The first is an elaborate model for aeolian sand transport proposed by Van Rijn and Strypsteen [45] which does include moisture content, vegetation and beach armoring by shells in a fairly simple form which is calibrated with wind-tunnel experiments. A second model is proposed by Hoonhout and De Vries [19] which is a numerical model and allows for the inclusion of varying sediment budget both spatially and temporally, called AeoLiS. This makes AeoLiS suitable for the computation of aeolian sediment transport in coastal environments, as in this study.

AeoLiS is a complex 2DH numerical modeling tool that incorporates various aeolian sediment transport processes to compute sediment transport and associated bed level change, for gentle slopes like dune profiles [19]. The main equation that is used by AeoLiS to simulate sediment transport is a two-dimensional advection equation,

see equation 4 adopted from De Vries et al. [46] and used by Pourteimouri et al. [1]:

$$\frac{\partial c}{\partial t} + u_{s,x}\frac{\partial c}{\partial x} + u_{s,y}\frac{\partial c}{\partial y} = E - D \tag{4}$$

Where c describes the sediment concentration in air [kg/m^2], u$_s$ denotes the saltation velocity in both x- (cross-shore) and y- (alongshore) directions [m/s]. The right-hand side (E - D) represents the net entrainment rate of sediment [kg/m^2/s].

Aeolian sediment transport is key for the formation of coastal sand dunes, though not much research has been performed on aeolian transport over a dune profile. Two studies found that the shape of dune formations causes reduced sediment transport over the dune toe and at the dune crest. An increase in sediment transport was found just upwind of the dune crest caused by changes to the wind field [14] [18]. In addition, Jonkheer [18] found that increasing incidence wind angle results in a significant reduction of sediment transport rate over the dune profile. The effects were largest at the dune crest. For increasing dune slope, the sediment transport rate at the dune toe showed a significant decrease. At the dune crest, a steeper dune resulted in a higher sediment transport rate. Furthermore, Jonkheer [18] has investigated the influence of vegetation by reducing the shear velocity with a factor of 1.5 at the location where vegetation is simulated. Their findings indicated that sediment transport is fully blocked at the dune toe, where the vegetation started in the model. Over the dune slope and at the start of the dune crest sediment transport still increased though was significantly smaller in magnitude, with a factor of approximately 5.

The placement of buildings on the beach influences aeolian sediment transport around the building as a result of alteration to the near-bed wind field. Stevers [17] and Hobeika [14] found that buildings affect sediment transport in duneward direction least if placed at 5 meters from the dune toe and if the building face is oriented towards the dominant wind angle. Besides, buildings could bend longshore winds in cross-shore direction resulting in enhanced sediment transport in duneward direction [17]. Pourteimouri et al. [16] proposed that gap spacing between buildings in a row can either limit or enhance sediment transport in downwind direction depending on wind incidence angle. In a more recent study, Pourteimouri et al. [1] found that sediment transport in duneward direction may be enhanced or reduced depending on the pole height of the buildings and the distance downwind from the building. This may be caused by reversed flow and/or a low-speed wind velocity region downwind of the building. For increasing pole height this region is located further downstream of the building. Besides, an appropriate gap width ratio between neighbouring buildings may enhance downwind sediment transport by flow acceleration as a result of funneling effects. For elevating buildings on poles, this effect may be created as well in the gap underneath the buildings. Effects of pole height on sediment transport were found to be largest directly at the downwind face of the building and reduce

further downwind of the building.

2.3 Bed morphodynamics around a dune profile and building geometry

Aeolian sediment transport can induce bed morphological evolution and on decadal time scale this may result in the formation of bedforms such as coastal sand dunes, as often observed along sandy beaches at coastal environments (e.g. [47]). These bedforms commonly have a slope of approximately 30 degrees, which is limited by the properties of the sand particles at the bed [48] [18]. Dunes may erode in short-term periods of storms (wind and waves) due to strong sediment entrainment compared to aeolian transport-driven dune growth which occurs during long-term periods of relatively calm weather conditions [47].

As previously mentioned, vegetation can often be found on coastal dune profiles. Vegetation cover is key to the existence of dunes since root systems stabilize the bed, reducing erosion of the bed. Besides, the reduction in bed shear stress caused by the presence of plants enhances sediment trapping and promotes dune growth [12]. Without the presence of vegetation, the dunes cannot effectively trap sediment over the dune slope and the crest of the dune would rapidly get eroded [49] [18]. Besides, the dune shape causes a region of sediment deposition upwind of the dune toe and over the dune toe, which is strongly influenced by the presence of vegetation [50] [18]. Just upwind of the dune crest, a decrease in deposition or potentially erosion may occur. Jonkheer [18] also found a region with deposition just downwind of the dune crest. The sedimentation patterns are strongest for a cross-shore wind (0°) and dune slope of 20° and decrease for varying parameters [18].

Research on the effects of a building on dune morphology is complex though multiple studies have been performed to investigate this [51] [9] [3] [15] [16] [1]. Generally, findings indicated that dune growth may be limited or enhanced depending on building characteristics, such as shape, size, construction material and placement. Studies by Poppema [15], who used field experiments, and Pourteimouri et al. [3] [16] [1], who used numerical modeling, performed research on the influence of building geometry, gap width between buildings that are placed in a row and pole height on sedimentation patterns around one or multiple buildings over a flat bed. The findings of these studies are discussed in the following paragraphs

Poppema [15] and Pourteimouri et al. [3] indicated that sedimentation patterns are generally one order of magnitude larger than building geometry, of which building width has largest influence on sedimentation patterns. Gap width showed large influence on sedimentation patterns, defined in terms of gap width ratio (gap width divided by building center to center distance). For gap width ratio smaller than 0.5 sedimentation patterns are similar to that of on very wide building. For larger gap width ratios, the patterns around two neighbouring buildings interact to form a com-

plex structure and showed dependency on gap width. This relation is valid up to a sufficiently large gap width ratio, after which patterns form without interaction between two neighbouring buildings. Poppema [15] and Pourteimouri et al. [16] found similar critical gap width ratios of 0.67 for patterns of neighbouring buildings to develop separately. The placement of buildings oblique to the incidence wind angle seemed to cause asymmetry in sedimentation patterns with a relation to this wind angle [15].

In addition, it was found that the placement of buildings on poles results in an expansion of the sedimentation pattern size [15] [1]. Pourteimouri et al. [1] indicated that the erosion region upwind of the buildings shifts to just underneath the building. Also, a region with strong erosion forms directly downwind of the building which is not found for buildings without poles. A deposition area behind the buildings is formed and the deposition tails behind the gaps spread over a longer distance without changing significantly in magnitude, indicating more deposition [1]. This contradicts somewhat with field observations by Poppema [15] who found deposition tails downwind of the building to be located further downwind, extending in size and decreasing in magnitude. Increasing pole height seemed to move the deposition tails further downwind [15].

A commonly used method to approximate morphological bed evolution over time is by means of the Exner mass balance equation [52] which is deduced from the original Exner equation [53]. The equation assumes that bed level change is proportional to the convergence of the sediment transport rate, see 5:

$$\frac{\partial z_b}{\partial t} = -\frac{1}{\rho_s(1-n)}\vec{\nabla}\cdot\vec{q} \tag{5}$$

Where z_b represents the bed level elevation in [m] and can vary on temporal scale t in [s]. ρ_s defines the sediment density in [kg m^{-3}], n the sediment porosity in [-] and q the sediment transport rate in [kg m^{-1} s^{-1}]. This mass balance provides that convergence of the transport rate results in a positive bed level change over time period t, thus sediment is being deposited. For a divergence of the transport rate, this is conversely and erosion of the bed occurs.

Though as discussed in chapter 2.2 sediment transport limiting processes are present in coastal environments. Since the Bagnold formula for sediment transport is based on a steady wind field and abundance in sediment supply, the morphological bed evolution in the field is generally overestimated. AeoLiS is able to compute bed level change including some of these sediment supply limitations [19]. Pourteimouri et al. [1] have compared these two methods. The coupled model generally computes less bed level change, especially underneath the building and downwind of the building. The direct use of the Bagnold equation results in much deposition underneath and downwind of the building whereas AeoLiS computes mainly erosion. Down-

wind of the building, both methods compute deposition, though AeoLiS computes much less deposition to occur. A strong difference between both methods is the strong gradient in bed level for the direct use of the Bagnold equation, which cannot be found in the results computed by AeoLiS [1]. This may be explained by the avalanche process in AeoLiS to avoid large gradients near strong erosion or deposition regions. Besides, the differences could be related to additional sediment supply limitations that are included in AeoLiS which are not included in the direct Bagnold method. This Exner method computes the maximum sediment transport which occurs if sand supply and fetch length do not limit sediment transport [1]. Also, local variations in wind velocity are included as well as non-linear processes which are known to decrease the amplitude of patterns in bed morphodynamics [1].

Since the coupling model as proposed by Pourteimouri et al. [1] has shown optimistic results with respect to field observations by Poppema [15], this model has the potential to simulate morphological bed evolution over the bed when including a dune profile in the domain. For that reason, the research of this thesis is performed using the coupling model as proposed by Pourteimouri et al. [1].

3. Methodology

This chapter discusses the various steps in the methodology to answer the research questions. Figure 4 shows how the research questions are related. The first part introduces the model setup, followed by an elaboration of the model which is used in this research. Next, a case is presented which introduces a row of beach buildings placed at the Zuiderstrand near Kijkduin. This case will be used for validation. The third section will elaborate on the choice of the variation in pole height and building location with respect to the dune toe. The last section discusses the step-wise approach which has been followed in this study.

3.1 Model setup

The building design has been based upon a row of beach buildings at the Zuiderstrand near Kijkduin, which is further elaborated in section 3.2. In addition, this study will be performed using a coupled model proposed by Pourteimouri et al. [1] since results were considered promising for the computation of bed morphological change around a row of buildings on poles placed on a flat beach in relation to field observations [15] [1]. Next, appropriate settings for the coupling, the airflow model OpenFOAM and the sediment transport model AeoLiS are elaborated. The model domain is presented first.

3.1.1 Model domain

A schematic visualization of the model domain can be found in figure 5. The parameters are provided in table 3.1 and will be elaborated hereafter. The length, width and height of the beach buildings are based on a row of beach buildings that have been placed on the Zuiderstrand near Kijkduin [54], see section 3.2. The row exists of 10 buildings on poles with certain height (H_{pole}) placed on the beach at a distance from the dune toe ($L_{building-dune}$). In the model, the geometry of these buildings is simplified into a cuboid shape taking into account the model resolution, see section 3.1.3. The dune profile is implemented as a simplified uniform single dune without longshore variations. Dunes generally include large spatial variation, however, this creates challenges for the implementation in the model. Therefore, the dune shape is designed according to the method used by Jonkheer [18] and based on the natural and common dimensions of a dune [48] to represent an average dune that can be found in the field. An elaboration of the dune shape can be found in Appendix D The placement of identical beach buildings in a row generally results in somewhat similar sedimentation patterns around the middle buildings of the row, see figure 11.

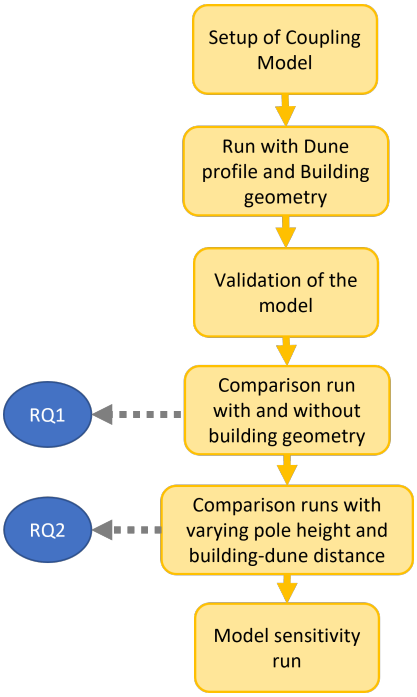

Figure 4: Schematization of the stepwise approach used to answer the research questions in this study

Therefore, computation time is reduced significantly by limiting the domain width to one building plot using circular boundary conditions (see section 3.1.3) as to represent a building plot in the middle of a row. In addition, domain height (H_{domain}), beach length (L_{domain}) and dune top length (L_{top}) are chosen to minimize the boundary effects in the domain, see Appendix E. Vegetation commonly starts approximately at the end of the dune toe with large spatial variation. However, the implementation of spatial variation is considered to be irrelevant due to the rather small domain width. Besides, interpretation of the model results could become challenging if vegetation starts at varying distances into the dune. Therefore, vegetation is included some distance into the dune ($L_{d,non-veg}$) with equal coverage over the domain width (W_{domain}) and stretches over the dune slope ($L_{d,veg}$) and dune top (L_{top}).

3.1.2 Coupling Model

As discussed in chapter 2.2, AeoLiS [19] is a complex sediment transport model that incorporates various processes to simulate sediment transport. AeoLiS is able to compute bed shear stress over a surface which is then used to compute sediment transport. Though this is valid only for a gently sloped bed, whereas buildings consist of vertical walls with sharp edges [1]. To compute the complexity of the near-bed wind field around buildings, Pourteimouri et al. [1] created a coupling between an airflow model in OpenFOAM, to compute the bed shear stress, and the aeolian sediment transport model AeoLiS.

The first step in the coupling is the computation of the airflow field within a three-

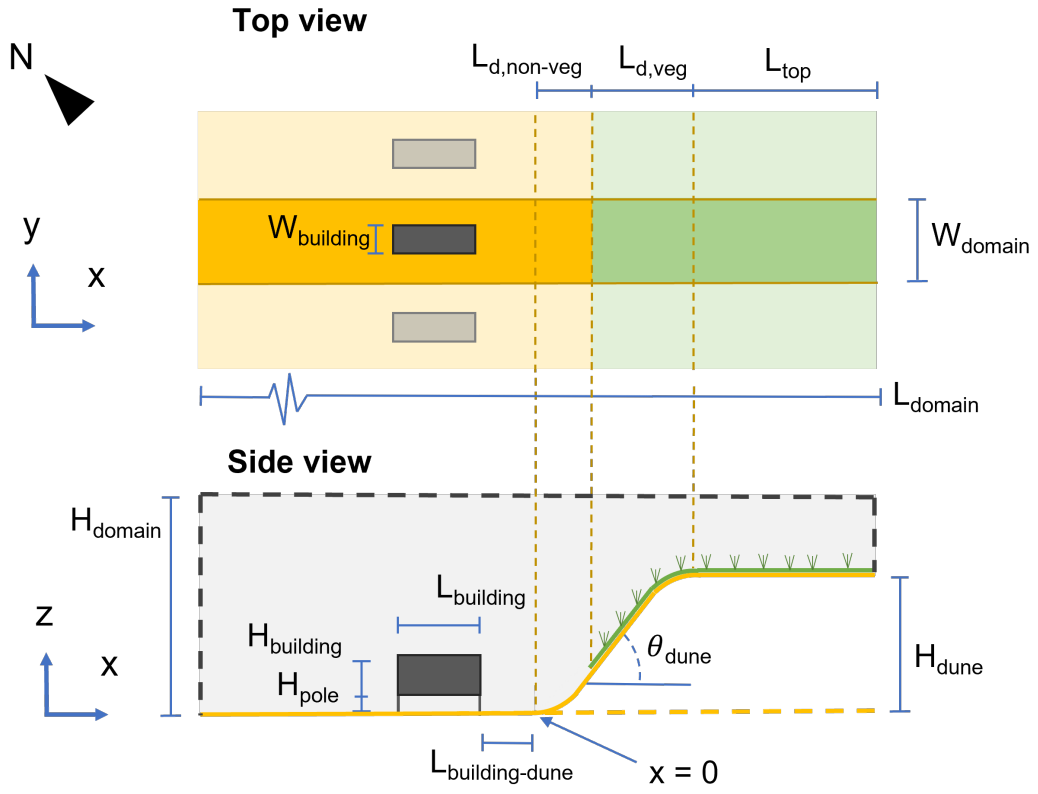

Figure 5: Schematized overview of the computational domain. The figure includes three model domains (in y-direction) to indicate that the model domain (dark shading) represents a single plot as part of a row of buildings.

Table 3.1: Model domain and building geometry. The design parameters of the buildings ($W_{building}$,$H_{building}$ and $L_{building}$) are based on the beach buildings near Kijkduin [54].

Variable	Value	Unit
L_{domain}	150.0	[m]
H_{domain}	40.0	[m]
$L_{d,non-veg}$	5.0	[m]
$L_{d,veg}$	17.0	[m]
L_{top}	53.0	[m]
W_{domain}	12.0	[m]
$W_{building}$	3.6	[m]
$H_{building}$	3.0	[m]
$L_{building}$	8.0	[m]
$L_{building-dune}$	To be determined	[m]
H_{pole}	To be determined	[m]
H_{dune}	10.0	[m]
θ_{dune}	30	[°]

dimensional domain using a steady-state wind model in OpenFOAM. The wind-induced bed shear stress over the surface is then extracted at the grid point locations in AeoLiS. The extracted bed shear stress is used by AeoLiS to compute the associated morphological bed evolution over a certain time period. Small changes to the bed cause little alterations to the wind field compared to the changes caused by the presence of a dune profile or a row of buildings. Though, over time bed forms may grow, as well as the influence on the wind field. To incorporate these morphologically induced near-bed wind field changes, the bed shear stress needs to be updated through OpenFOAM after a certain time period. The updated wind field is again exported to Aeolis to compute morphological bed evolution. An overview of the coupling model can be found in figure 6.

3.1.3 Model settings

OpenFOAM settings

Since results from the study by Pourteimouri et al. [1] showed promising results, similar OpenFOAM settings are used in this study. The SimpleFOAM solver is chosen which uses the Finite Volume Method (FVM) and Pressure-Linked Equations (SIMPLE) to solve the Reynolds-Averaged Navier Stokes equations. To capture the complex turbulent flows around the buildings and over the bed, the k-ϵ turbulence closure model is utilized. The solver and closure model are not further investigated in this study. The parameter settings for the model can be found in Appendix B.1.

A mesh is set up with the automated meshing utility 'cfMesh' with the finest cells of size $\Delta x = \Delta y = \Delta z = 0.05$ m adjacent to the buildings on poles and $\Delta x = \Delta y = \Delta z = 0.10$ m over the bed to capture the wind field around the building and over the bed with high quality. The mesh expands away from the surface to reduce computation time. The coarsest cell size $\Delta x = \Delta y = \Delta z = 1.60$ m is used far from the buildings and bed surfaces. The domain height is set to 40 meters. Since the wind field is restricted by the continuity of incompressible flow, wind velocity increases over the dune profile (10 meters in height) with a factor of 40/30 = 1.33. To properly account for these effects, domain height should be reconsidered for a different dune height. This grid composition creates a mesh with approximately 2.3 million cells. A side view can be found in figure 7.

The lateral boundaries in OpenFOAM are set to the periodic boundary condition, 'CyclicAMI'. This ensures that flow conditions at both sides are similar, to allow interaction of the wind at both sides of the building to represent the wind field around a row of buildings. CyclicAMI requires equal patches though allows dissimilar inner grid composition. Unequal side patches form due to asymmetry in morphological bed level change over time as computed by AeoLiS. To ensure equal lateral patches, a correction of the bed very close to the lateral boundaries is performed, see Appendix C. The top patch is defined as slip and the bed and building surface as no-slip. The outlet is defined as zero gradient.

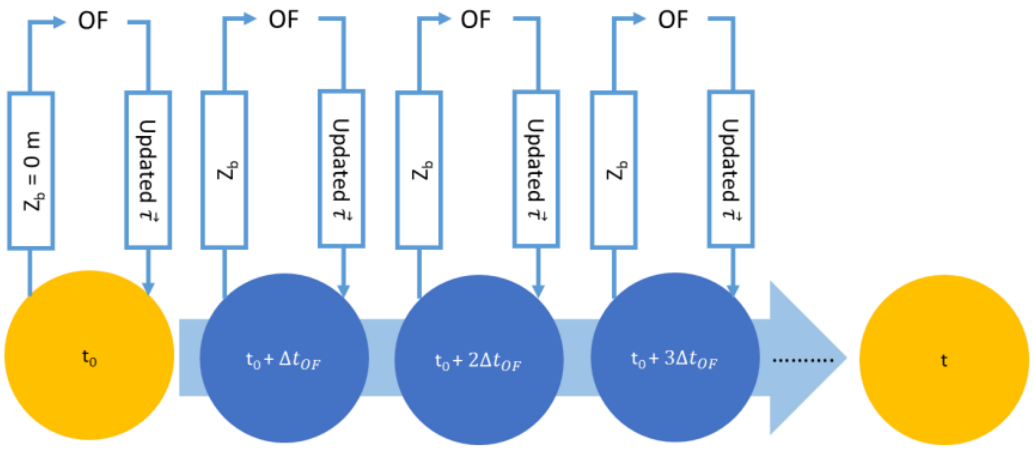

Figure 6: Overview of Coupling model adopted from Pourteimouri et al. [1]. It shows the iterative process over time between multiple wind field computations through OpenFOAM and bed updates through AeoLiS.

The inlet patch enforces wind conditions into the domain using an Atmospheric Boundary Layer (ABL). This ABL is defined by a vertical logarithmic velocity profile, turbulent kinetic energy and dissipation. The enforcing wind direction is North-Western (x-direction in figure 5) and the reference wind speed (U_z) is set to 17 m/s at a reference height (z_{ref}) of 1.8 m. The wind is chosen orthogonal with the front face of the building due to limitations in the version of the AeoLiS model that is used in this study. The wind speed of 17 m/s is above average [55] and can be considered as a storm on the scale of Beaufort [1]. This high wind is chosen to speed up the morphological bed evolution process. In addition, the uniform roughness height of the bed (z_0) is set to 1x10^{-5} m, which is based on median grain size at the beach ($300\ \mu$m) [1].

Coupling settings

The coupling computes morphological bed evolution over a time period of 24 hours (1 day) due to the high computational cost of the coupling model. In addition, a wind speed of 17 m/s generally occurs for a period no longer than one day [55]. The number of wind field updates through OpenFOAM is set to 6 times within this 24 hour period. As a result, changes in the bed form are captured in the wind field every 4 hours. This choice is based upon the ability to divide the total simulation time by this time step and the frequency is slightly higher compared to Pourteimouri et al. [1], which showed promising model results for an update of the wind field every 5 hours.

AeoLiS settings

The 2D horizontal grid in AeoLiS is defined with a cell size of $\Delta x = \Delta y = 0.20$ m to correctly capture the grid points of the dune shape, see section D. The elevation

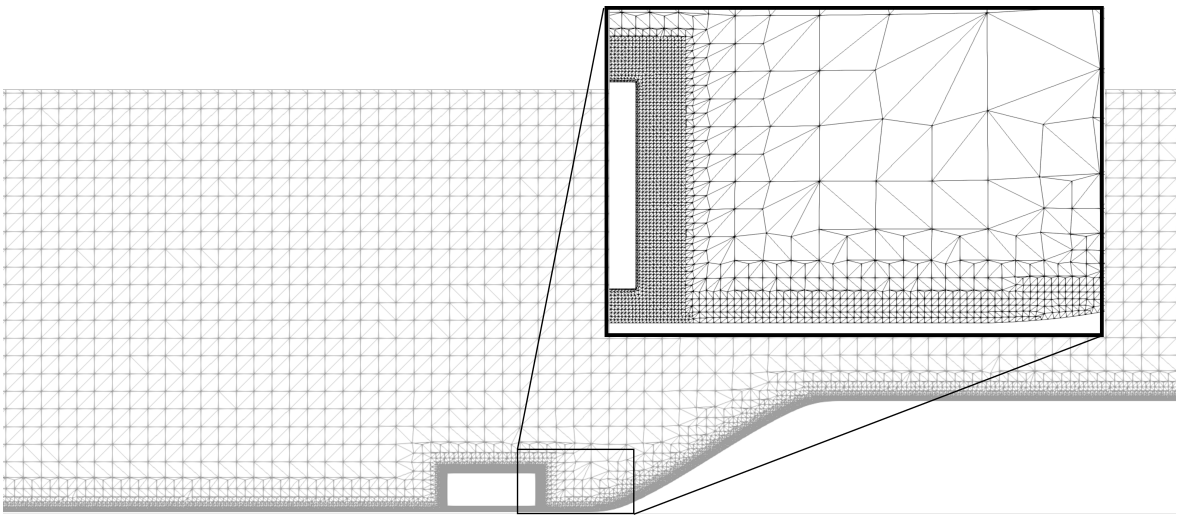

Figure 7: Cross-sectional view of the mesh composition near the building geometry and dune profile in cross-shore direction. The building poles are not visible since these are placed underneath the corners of the building, whereas this figure shows a cross-sectional view in which the building corners are not included.

data is provided for each cell in the computational domain as well as the bed shear stress computed by OpenFOAM. All settings for the AeoLiS model are provided in Appendix B.2

Sediment supply limitations have not been included in the coupling model yet [1]. Thus for appropriate implementation of the effects, additional research is required into the various sediment supply limitations. Due to time restrictions, it has been decided to implement the environmental conditions to represent an abundant supply of dry sediment, with a simple implementation of vegetation as sediment supply limitation over the dune slope and dune top. The dry supply of sediment is represented by a non-erodible layer at a depth of 4 meters and no moisture throughout the bed. The bed consists of sand particles with a size of 300 μm which is common along the coast. The lateral boundaries are defined as circular conditions such that the domain represents a single plot of a row of buildings, though may only be applied for a grid that is aligned with the wind direction [56]. Additionally, AeoLiS includes an avalanche process to limit strong gradients in bed-level elevation, for example near the poles. The angle of repose is set to 34° [57]. This limits the maximum dune angle in AeoLiS, since the avalanching process occurs for slopes steeper than the defined angle of repose.

The presence of vegetation has a significant impact on aeolian sediment transport over a dune profile, see section 2.2 and 2.3. AeoLiS allows to include effects of vegetation as vegetation cover for each cell in the grid. The coverage is then used to reduce the bed shear stress with a factor. In this study, a vegetation cover of 20 percent is included over the dune profile, which results in a reduction of bed

shear stress with a factor of approximately 2. This is somewhat arbitrary, though is comparable to the reduction factor used by Jonkheer [18] (1.5).

3.2 Model validation case

To improve understanding of the validity of the model for the computation of bed morphological evolution over time around a row of beach buildings placed close to a dune profile, a validation is performed. The validation involves elevation data that has been collected around beach buildings on the Zuiderstrand near Kijkduin in the Netherlands, see figure 8. The project includes the placement of various rows of beach houses, though this section will focus on a specific row of beach houses only, see figure 8 highlighted with a black arrow. The municipality of The Hague has provided permits for the placement of these beach houses over a period of 5 years between the 1st of March and the 1st of November. This row of beach buildings can be used for the validation of this study since information on the design and placement of the row of buildings is available, the buildings are placed on poles and at relevant distances from the dune toe and elevation field data is available.

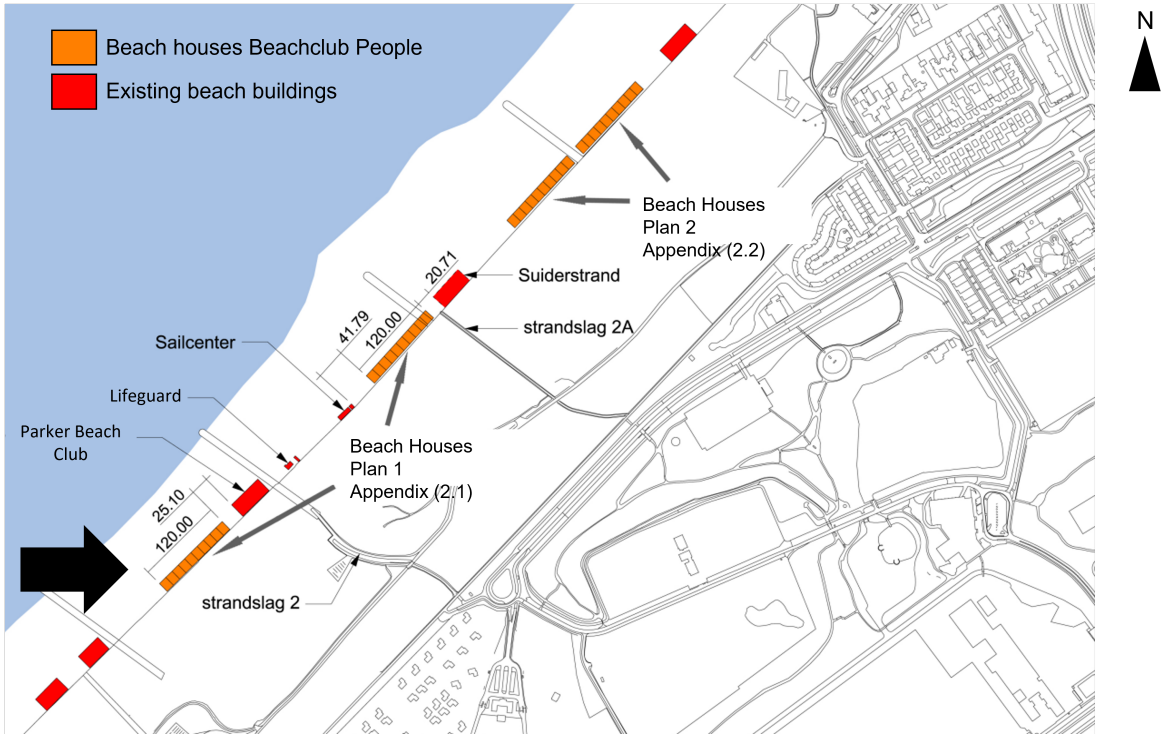

Figure 8: Overview of the Zuiderstrand near Kijkduin, the Netherlands [5]. The specific row beach houses that is used in this study is highlighted with a black arrow.

Since the project is located in the vicinity of the Natura-2000 reserve Solleveld & Kapittelduinen, the buildings need to comply to various design conditions [54]. The buildings Therefore, The design and placement of the beach buildings are intended to minimize the environmental effects in the vicinity of the buildings. The project has

been tested on various environmental indicators, such as surface area loss, noise disturbance and light disturbance [54]. However, the following part considers the sand deposition and excavation (flattening of the beach prior to building placement) indicators only.

The row of beach buildings consists of 10 buildings placed on a plot of 12 meters width and have a length of 10.0 m, a width of 3.5 meters and a height ranging between 2.90 and 3.50 meters, see figure 9. The buildings are placed with a spacing of 8.5 m [54], which is considered to be sufficient to minimize the interaction of the wind fields and effects on sediment transport since the minimal gap width is estimated to be the width of the building [58]. However, the presence of buildings may still enhance erosion directly downwind of the building and affect sediment transport and deposition up to 25 m downwind of the buildings [59]. The buildings are placed 5 meters from the fence along the dune toe on poles with the height ranging between 0.50 and 0.80 meters. The building-to-dune distance is considered to be sufficient to allow estimated dune growth over the period during which the buildings are placed on the beach [60]. Potential effects of the buildings may recover over the winter period when the buildings are removed since wind speed commonly increases [55] during the winter enhancing the natural recovery process of the dune system. It has been decided to place the buildings with the front face pointing towards the dominant wind direction (NorthWestern [55]) to minimize wind field alteration [54]. However, this cannot be included in the model since the version of AeoLiS is not able to deal with oblique wind angle, see section 3.1.3. The translation of the building design parameters into the model can be found in table 3.2.

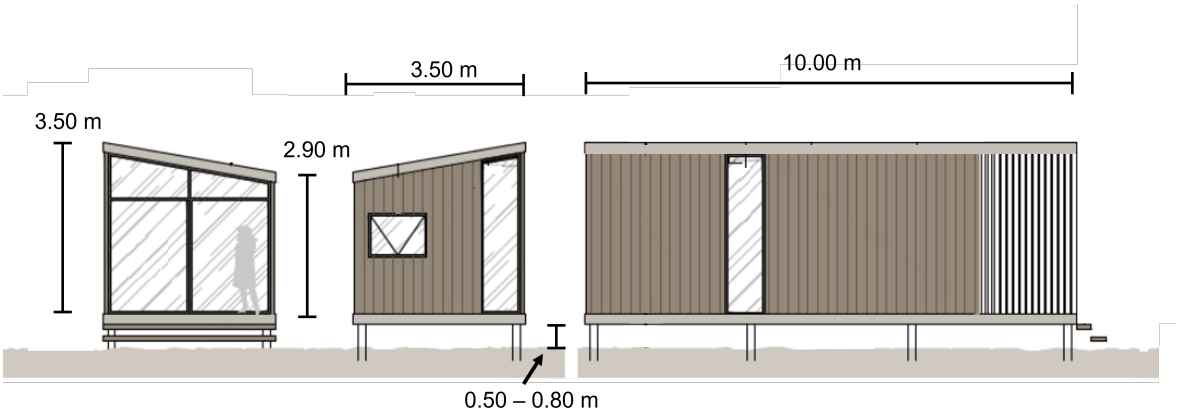

Figure 9: Design beach buildings Kijkduin, the Netherlands [6]

In support of the ShoreScape project, Shore Monitoring & Research collected data to monitor the Zandmotor between Kijkduin and Ter Heijde using a UAV LiDAR system. The data captures the area around the row of beach buildings as indicated in figure 8. The elevation data includes sedimentation patterns that are created by the presence of the row of beach houses as well as by the environmental conditions that occurred prior to the data survey [7]. The data surveys were performed on the

Table 3.2: Model domain and building geometry similar as table 3.1 with $L_{building-dune}$ and H_{pole} specified for the validation case.

Variable	Value	Unit
L_{domain}	150.0	[m]
H_{domain}	40.0	[m]
$L_{d,non-veg}$	5.0	[m]
$L_{d,veg}$	17.0	[m]
L_{top}	53.0	[m]
W_{domain}	12.0	[m]
$W_{building}$	3.6	[m]
$H_{building}$	3.0	[m]
$L_{building}$	8.0	[m]
$L_{building-dune}$	5.0	[m]
H_{pole}	0.5	[m]
H_{dune}	10.0	[m]
θ_{dune}	30	[°]

10th of July 2017 [7] and on the 9th of October 2018 [61]. This data is processed to perform the validation with respect to model results.

For the comparison of the field data at Kijkduin with model results, the elevation data is being processed. The data includes the bed level elevation with a resolution of 0.25x0.25 and 0.5x0.5 cm around the row existing of 10 beach buildings. Since the elevation data might include local variation as a result of people altering the environment or minor variation in environmental conditions, the elevation data of all plots is combined to represent one building plot o represent the most reliable validation data. However, sedimentation-erosion pattern around the outer buildings of the row deviates from the middle buildings due to the interaction of the wind field with only one neighbouring building. To exclude the side effects, the plots of the two outer buildings on both sides of the row are excluded from the data analysis. As a result, the average bed level elevation is computed for the six buildings in the middle of the row to represent bed morphology around a row of buildings placed at a distance of 5 meters from the dune on poles with a height of 0.5 meters.

The buildings of both field surveys are placed roughly at the same location. The starting bed morphology has a significant effect on the sedimentation patterns that form around the buildings, though is unknown. However, the buildings are removed over the winter period, allowing the bed morphology to recover. Therefore, it is assumed that the starting bed morphology did not differ between both years. The evolution of the bed thus corresponds to the time period over which the buildings have been present on the beach. The data of 2017 is observed 3 months prior to the data of 2018, allowing sedimentation patterns caused by the presence of

buildings to develop over a period of 3 months longer compared to the data of 2017. Also, sediment transport is mainly influenced by wind direction and velocity, though detailed wind data is not available at Kijkduin over the relevant periods. Therefore, it is assumed that the sedimentation patterns are caused by the dominant wind incidence angle, which is West [55].

3.3 Model configurations

To answer the research questions various model configurations will be computed. The first research question investigates the influence of a row of buildings on poles placed in front of a dune profile on sedimentation patterns over the dune profile. Therefore, two model configurations will be computed. At first, a run will be performed which does not include a building geometry, referred to as the 'No Building' case. This case represents undisturbed morphological bed evolution induced by a dune profile. The second model configuration is based on the beach buildings at the Zuiderstrand near Kijkduin, which has been described in section 3.2, with parameter settings as presented in table 3.2. The building is placed on poles of 0.5 meters and at a distance of 5 meters from the dune toe and is referred to as the 'Default Building' case.

The second research question addresses the influence of pole height underneath the building (H_{pole} in figure 10) and the distance between the building and dune toe ($L_{building-dune}$ in figure 10) on bed morphology. Both parameters are varied and the selection for both parameters is well-considered due to time limitations and high computational cost for each run. Pourteimouri et al. [1] showed influence on aeolian sediment transport for a pole height ranging between 0 to 2.5 times building width (H_{pole}/w). Considering a building width of 3.6 m in our study, usage of a similar range would result in uncomfortable high buildings and unrealistically large poles in relation to building dimensions and dune height. Besides, the largest effects on downward sediment transport were found for a pole height up to 0.8 times the building width [1]. In practice buildings often can be found either on the bed or on poles with a closed-off gap underneath the front face of the building, see figure 1 b. Therefore, the decision is made to create configurations with H_{pole} of 0.0 and 3.0 m. In addition, runs will be performed for a pole height of 0.5 m (Kijkduin case) and 1.5 m to get improved understanding of a potential relationship.

The placement of the beach buildings at the Zuiderstrand near Kijkduin is based on an estimate of dune growth over the period during which the buildings are present on the beach, which is estimated on 5 meters [54]. In addition, for the range of pole height ratios of 0 to 0.8, as decided upon in the previous paragraph, Pourteimouri [1] showed that sediment transport is significantly altered up to and including a distance of 4 times the building width. In our study this distance corresponds to approximately 14 meters, considering a building width of 3.6 m. To capture an extreme case, configurations will be performed for a larger distance of 20 meters. Another extreme

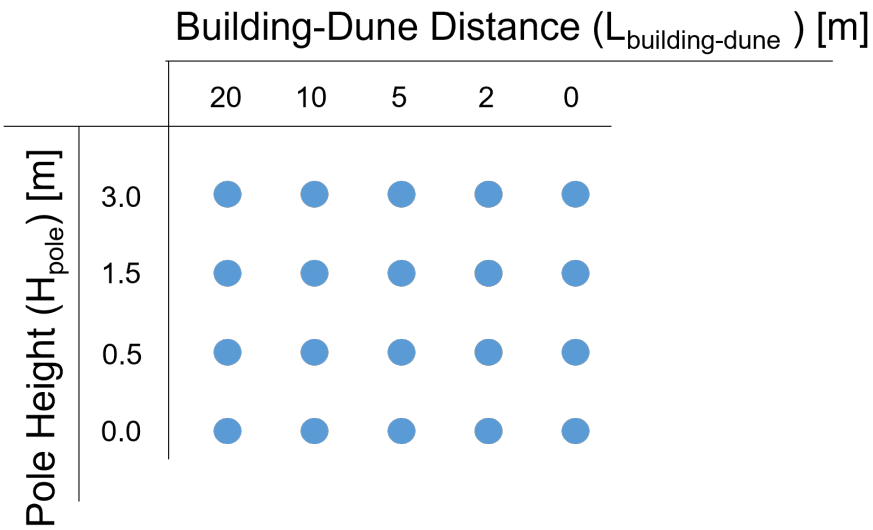

Figure 10: Overview of the configurations with varying the pole height (H_{pole}) and building-dune distance ($L_{building-dune}$) for the parameters in table 3.1. Additionally, a configuration, named 'No Building', is computed that does not include a building geometry to represent the undisturbed conditions. This configuration is not shown in the figure. Note that the difference between the parameters is not constant.

case is the placement of buildings directly at the dune toe (0 meters). Additional distances of 2 and 10 meters provide insight into the trends that occur between the previously described distances. This leads to a set of building-dune distances of 0, 2, 5, 10 and 20 meters. An overview of all 20 configurations, excluding a configuration without buildings, can be found in figure 10

At last, additional model runs will be performed to get insight into the sensitivity of certain model settings, since some model settings are decided upon in an arbitrary manner and might affect results significantly. At first, a configuration without the presence of vegetation is performed to get better insight into the influence of the implementation of vegetation, namely this method has not been studied extensively. Also, a configuration is performed with a domain height of 80 meters. Next, a configuration included lower wind velocity and lastly a different frequency for the wind field update through OpenFOAM. The results are analyzed on a dimensionless spatial scale to get insight into general behaviour rather than for a specific case by dividing with the building width, which is not varied throughout this study. This building design parameter was found to affect morphological bed evolution patterns the most and has been used in previous research for the conversion to dimensionless parameters.

4. Results

In this chapter, the results will be analyzed as described in chapter 3. At first, the data of the beach buildings at Kijkduin are processed and interpreted. In the second and third sections, varying building-to-dune distance and pole height are analyzed based on morphological bed evolution over the dune and around the building. The morphological bed evolution is used to create sedimentation patterns with respect to the initial bed (Z_{b0}). Next, an analysis is performed for a combination of varying building-dune distance and pole height. At last, certain additional model settings are varying in order to get better understanding of the sensitivity of these settings. It is important to notice that all spatial parameters on the axis of the figures are divided by the building width (w), 3.6 m to create dimensionless parameters, see section 3.3. The dune toe is considered to be the middle of the domain (x=0).

4.1 Validation data analysis

Figure 11 shows the elevation data around the row of beach buildings only for the survey that was performed on the 10th of July 2017. It can be seen that the sedimentation patterns around the middle buildings are indeed roughly similar. The red section in the South Eastern part of figure 11 is considered to be coastal dune. The buildings at the sides of the row show an exception to the sedimentation patterns since these only have one neighbouring building.

The data of figure 11 has been processed for observation on the 10th of July 2017 and can be found in the top subplot of figure 12 and will be referred to as 2017. The elevation that is measured on the 9th of October 2018 can be found in the bottom subplot of figure 12 and will be referred to as 2018.

Generally, the height of sedimentation patterns that occur around the building is in the order of 10^{-1} meter. The rather uniform high bed level elevation that is observed in front of the building is related to the presence of a path of concrete slabs. It can clearly be seen that the dune has extended seaward in the 2018 data while this pattern is significantly smaller in magnitude for the data from the year 2017. Besides, the limitation of dune growth caused by the presence of a row of buildings can clearly be seen in the data of 2018. Generally both subplots in figure 12 an erosion region forms at both sides of the front face of the building. Besides, behind the building a region forms with no deposition, indicating limitation of deposition compared to the region in between the buildings. Upwind of the building, considering the dominant wind direction is West, a region of deposition can be found. In the data of the year

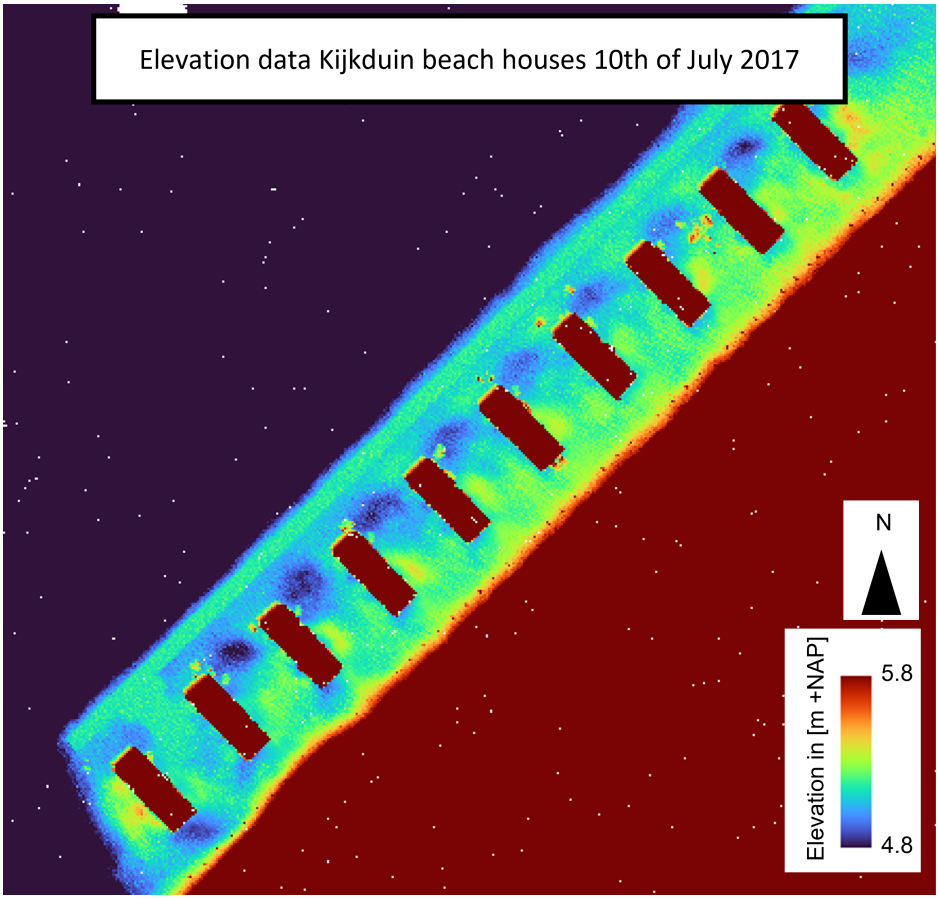

Figure 11: Elevation data Kijkduin beach houses measured on the 10th of July 2017 [7]. The elevation data is shown in the range of 4.8 - 5.8 [m+NAP].

2017 a deposition area can be found at one side of the building directly next to the side, which is not visible in the data of 2018. This may be formed depending on specific wind characteristics prior to the observation, whereas this did not occur prior to the observation of 2018.

4.2 Influence of a row of buildings on poles on dune morphodynamics

This section compares the model results of a configuration without a building ('No Building') and a configuration with a building ('Default Building'). Black dashed bars show the location of the dune toe (x/w = 0 [-]) and dune crest (x/w = 6.11 [-]). The building location and geometry is visualized with a black dashed box and the buildings are placed at building-to-dune distance ratio (D* = $L_{building,dune}$/w) of 1.39 [-] with a pole height ratio (P_h* = H_{pole}/w) of 0.14 [-].

Figure 13 shows sedimentation patterns for both the 'No Building' (a.) and 'Default Building' (b.) cases. It is clearly visible that the presence of a row of buildings on poles forms a horseshoe-like erosion pattern around the upwind side of the build-

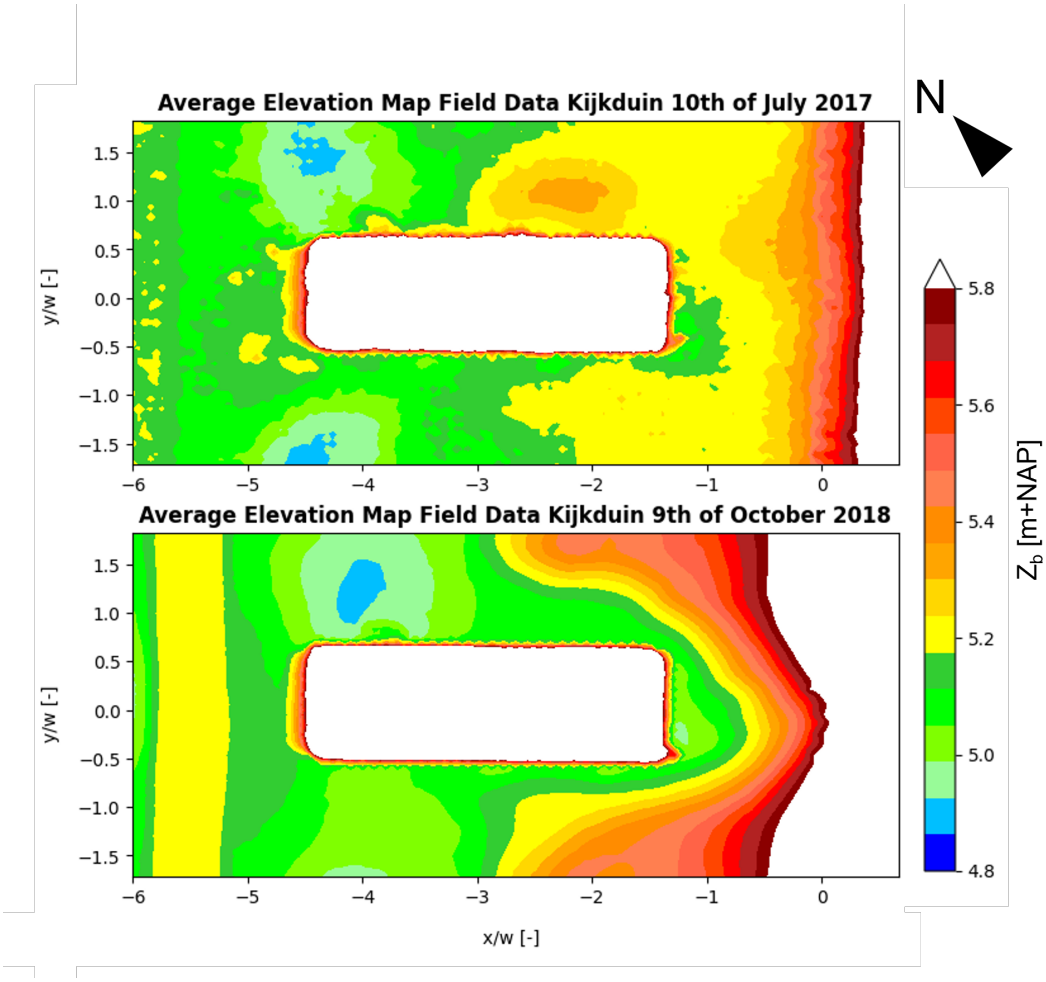

Figure 12: Elevation data Kijkduin beach houses measured on the 10th of July 2017 (top) and the 9th of October 2018 (bottom) [7]. The buildings are located in the middle of the figures and are colored white. The white section on the right-hand side of the figures indicates the higher elevation of the dune. The elevation data is shown in the range of 4.8 - 5.8 [m+NAP]

ing approximately 0.8 m deep. Directly downwind of the erosion tails, areas with strong deposition form approximately 0.6 m high. Underneath the building, a region with deposition can be found, whereas weak erosion can be found underneath the downwind face of the building.

To add to the visual analysis of the sedimentation-erosion patterns, the mean bed level change and its maximum and minimum (referred to as amplitudes) are computed over the domain width (y-direction) and are visualized in figure 14. It can be seen that the dune shape with a slope of 30 ° (blue) causes deposition upwind of the dune toe and erosion at the dune crest with small variation in amplitudes. Just downwind of the dune crest, some minor deposition and erosion can be found. Sedimentation over the straight section of the dune slope is minimal and shows no variation. In Appendix E the 'No Building' case is provided with a smaller range

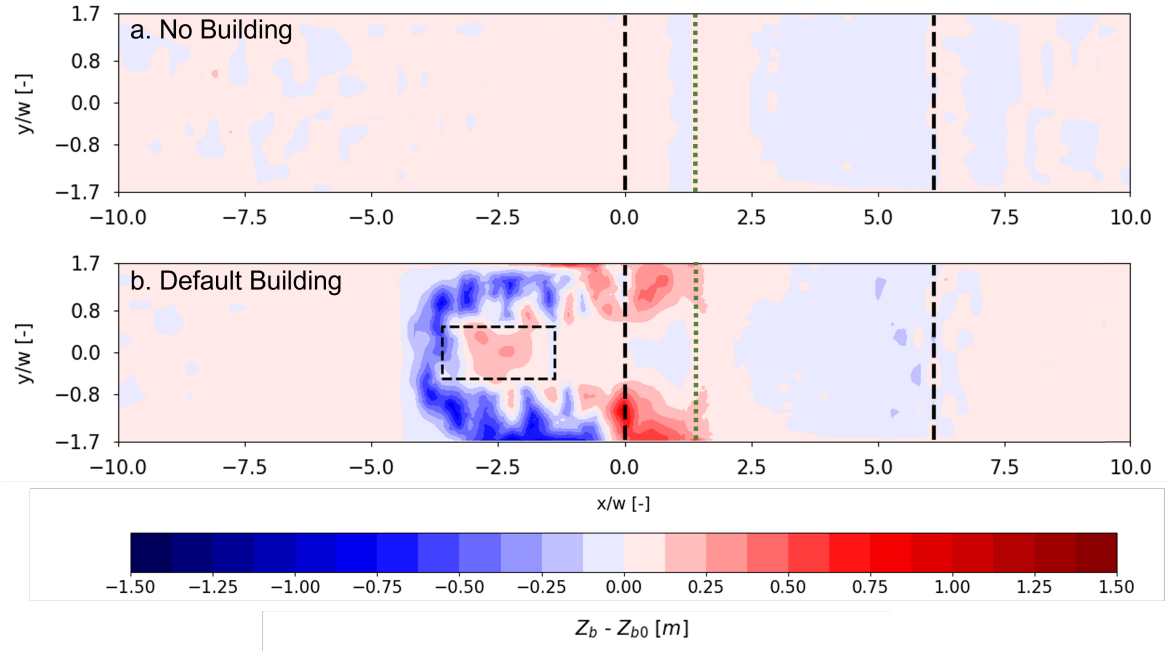

Figure 13: Sedimentation pattern (Z_b - Z_{b0}) for the cases a. 'No Building' and b. 'Default Building' over 24 hours. The black dashed box represents the location of the building geometry, the black dashed lines represent dune toe and dune crest. The green dotted line represents the start location of the vegetation cover.

for the y-axis (Z_b - Z_{b0}) to provide better insight into the patterns that are formed as a result of the dune shape. With the introduction of a row of buildings in front of the dune (red), a region of deposition is located far upwind of the buildings with similar magnitude of the deposition that occurs just upwind of the dune when there are no buildings ('No Building case'). Around the buildings, strong erosion can be found with significant difference between the amplitudes. At a moderate distance downwind of the building (D* = 1.0 [-]) a region is located with strong deposition. This region partly overlaps with the dune toe. Over the dune toe, just upwind of the vegetation, an increase in sedimentation height can be found, which decreases to zero further up the dune slope. At the crest of the dune, it can be seen that erosion is enhanced and variation in bed level change increases. Also, it can be seen that sedimentation height and difference in amplitude at the vegetated region are significantly smaller compared to the unvegetated area around the building.

4.3 Influence of building-dune distance and pole height on bed morphodynamics

Similar to figure 13, visualizations have been created for the sedimentation patterns over the bed and dune profile for all configurations discussed in chapter 3. Though, a clear comparison between the different configurations is rather difficult to make

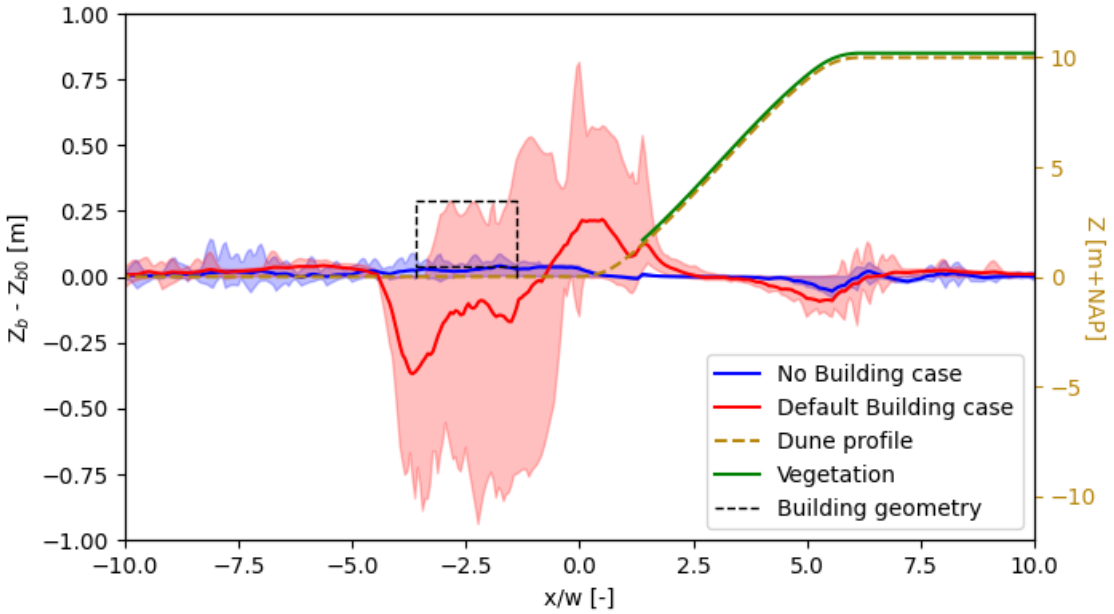

Figure 14: Average bed level change over the width of the domain for the 'No Building' (indicated by blue) and 'Default Building' (indicated by red) cases over 24 hours. The minimum and maximum amplitudes over the width of the domain are included and indicated by the shaded colors. The building geometry, dune profile and the location of vegetation are included in the figure

since the figures do not provide clear insight into the effects on bed morphology over different sections of the dune. Therefore, supporting figures are provided that quantify morphological bed evolution over different regions into average bed level change and the minimum and maximum amplitudes over the region. To get better insight into the influence of a row of buildings on bed morphology, the bed level change per region is shown relative to the 'No Building' case. Positive values indicate an increase in either average, maximum or minimum regional bed level height compared to the case without the presence of a row of buildings. First, the influence of distance between the building and dune is studied, followed by the influence of pole height. Afterwards, results are shown for combined variation in building-dune distance and pole height. The definition of the regions are shown in figure 15. The section between regions 1. and 4. are not included since the cross-shore length varies for different building-dune (D*) distance ratios and becomes zero if the buildings are placed at the dune toe. Besides, the aim of this study is on dune morphology, of which the most relevant regions are captured by this division of regions.

4.3.1 Influence Building-Dune distance

In figure 16 a. it can be seen that the dune toe is the most affected dune region as a result of the placement of a row of buildings. In addition, both the dune toe and dune

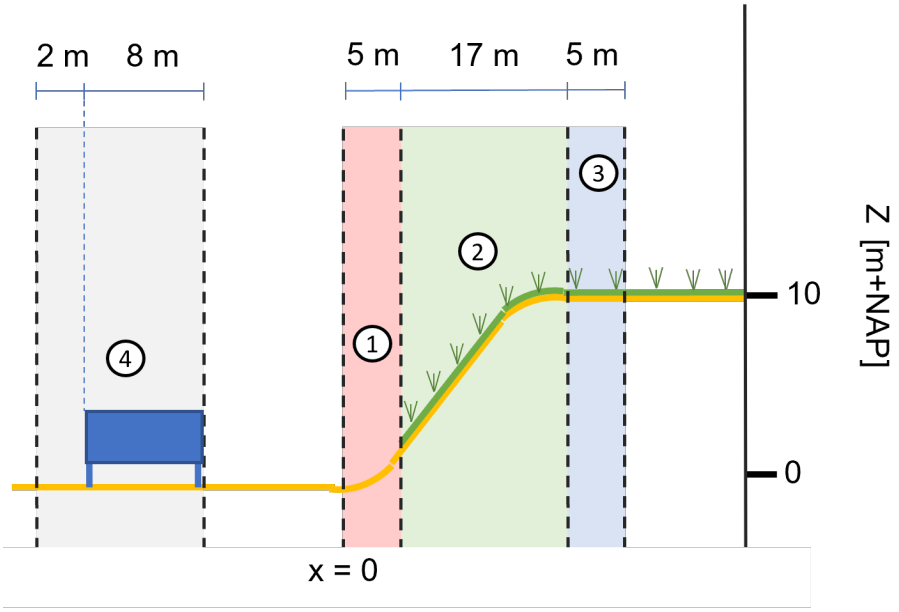

Figure 15: Schematized overview of regions in which morphological bed evolution will be analyzed. These regions include: 1) 'Dune toe', 2) 'Dune slope' 3) 'Dune top' and 4) 'Building'. The area between the building (4.) and dune toe (1.) regions differs for varying building-dune distance ratio (D*) and has not been included in any of the regions.

top show a positive relative mean bed level change, which is approximately zero or slightly negative for the dune slope. This indicates enhanced deposition over the dune profile as a result of the placement of a row of beach buildings which is maximum for buildings placed at moderate distance (D* = 2.8). Besides, all dune regions show a trend to zero mean relative bed level change for an increasing building-dune distance (D*), larger than 2.8 [-]. Over the dune toe region, increasingly less sediment deposits as the building is placed closer to the dune. If the buildings are placed at the dune toe (D* = 0 [-]), the mean bed level change shows a minor increase over the dune slope and top, whereas a strong decrease can be found at the dune toe. The relative erosion around the building shows a somewhat similar, but negative, trend as for the dune toe region. However, the magnitude of the relative mean bed level change around the building is significantly larger in magnitude.

In figure 16 b., it can be seen that the minimum amplitude remains rather constant for varying distance in all regions except the dune toe where deeper holes form for placement of the buildings closer to the dune. Near the building, largest variation in amplitudes can be found. The maximum amplitude of the relative bed level change at the dune toe, shows a similar trend as for the mean in that region, see figure 16 a. Also, the maximum amplitude for the dune slope and building region show a similar positive trend for placement closer to the dune. However, effects of varying the distance seem to have largest effect when the building is placed close to the dune for the dune toe, dune slope and area around the building.

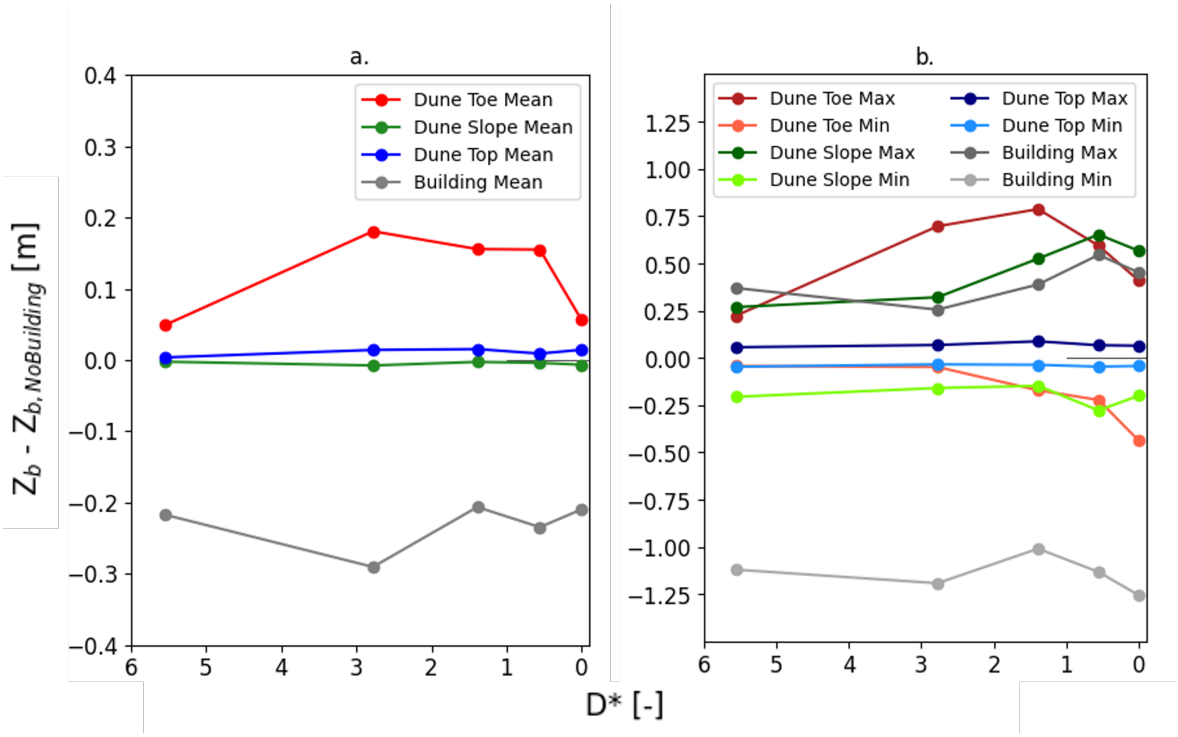

Figure 16: Influence of building-dune distance ratio (D*) on regional mean (a.) and minimum and maximum (b.) bed level change relative to the 'No Building' case over 24 hours. Building-dune distance ratio varies between 0 and 5.56 [-] for a constant pole height ratio (P_h*) of 0.14 [-]. The regions include: Dune toe (red), Dune slope (green), Dune top (blue) and Building (grey).

In addition, the subplots in figure 17 show sedimentation patterns for constant pole height ratio (P_h*) of 0.14 [-] and varying building-dune distance. It can be seen that undisturbed deposition tails form downwind of the building extending over a distance of approximately 4w (subplot e.). However, deposition tails are limited in magnitude and extend up to approximately 1.5w into the dune as the buildings are located closer to the dune toe (figures 17 b. and c.). For placement of the buildings directly at the dune toe, the deposition tails reduce significantly in magnitude (figures 17 b. and c.). The behaviour of the deposition tails supports the trend over the dune toe region in figure 16 a.

4.3.2 Influence Pole Height

In figure 18 a., it can be seen that the overall dune toe and dune top regions capture sediment, whereas the dune slope region erodes. For all dune regions, the relative mean bed level change is less when the buildings is placed on small poles (P_h* = 0.14 [-]) compared to placement on the bed (P_h* = 0 [-]). The deposition over the dune toe increases with increasing pole height. The dune slope and dune top region show least relative mean bed level change for a pole height ratio of 0.42 [-

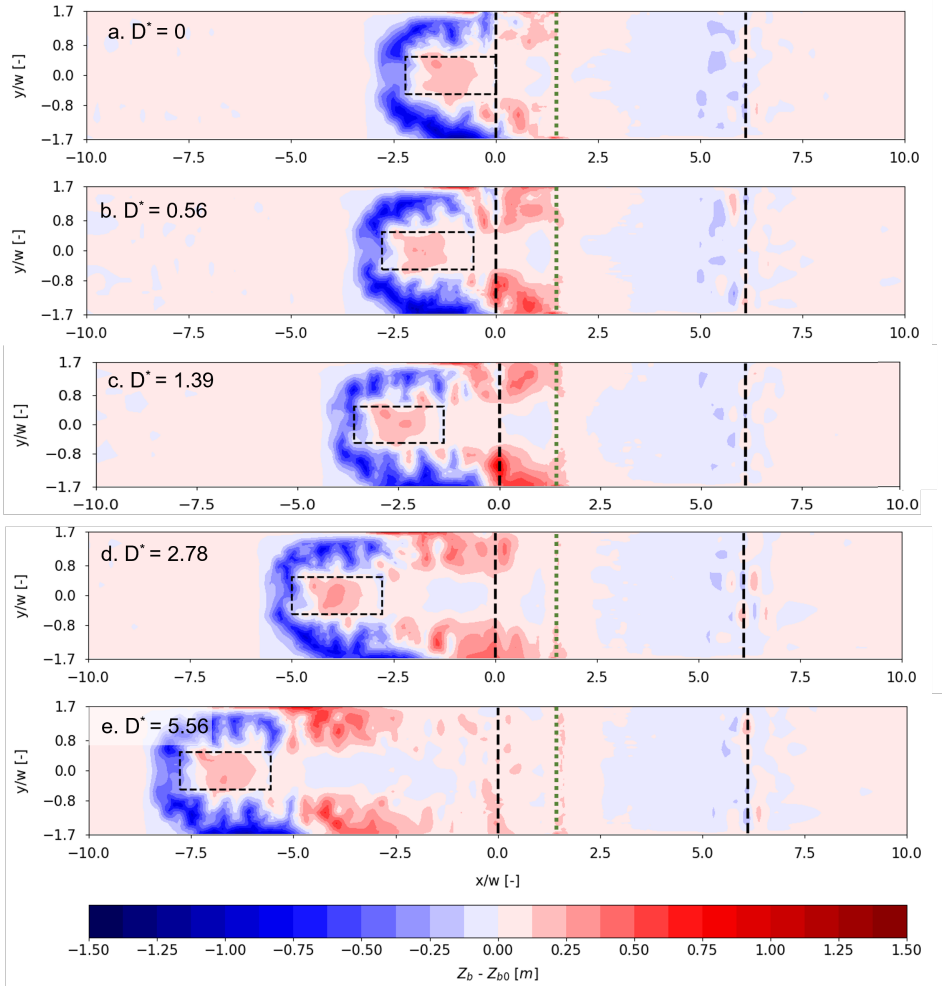

Figure 17: Sedimentation patterns (Z_b - Z_{b0}) over 24 hours for the configurations with increasing distance ratio: a. 0; b. 0.56; c. 1.39 ('Default building'); d. 2.78.; e. 5.56 [-]. All configurations include a pole height ratio of 0.14 [-].

] which increases for larger poles. However, the magnitude is significantly less in relation to the dune toe region. In the vicinity of the buildings, erosion occurs for all different pole height configurations with increasingly more erosion for increasing pole height. This enhanced erosion transports increasingly more sediment downwind, which could explain the increase of deposition for longer poles over the dune toe region.

The maximum and minimum amplitude of the relative bed level change over the four regions can be found in figure 18 b. In general, pole height variation shows small effect on both minimum and maximum amplitudes over all regions. Over the dune toe, dune top and building regions, the difference between amplitudes is smallest for buildings without poles (P_h* = 0), whereas this is true for the dune slope for medium long poles (P_h* = 0.42 [-]). Over the dune toe, the difference between the amplitudes reduces if buildings are placed on medium poles (P_h* = 0.42 [-]) compared to short

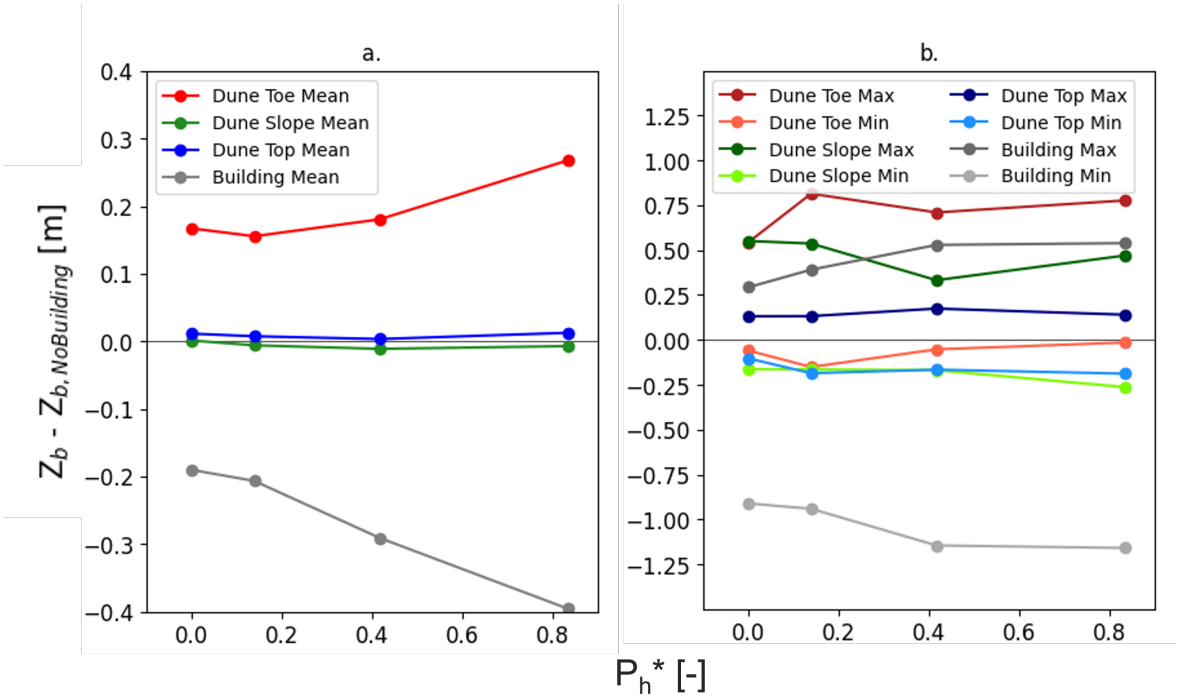

Figure 18: Influence of pole height ratio (P_h*) on regional mean (a.) and minimum and maximum (b.) bed level change relative to the 'No Building' case over 24 hours. Pole height ratio varies between 0 and 0.83 [-] for a constant building-dune distance ratio of 1.39 [-]. The regions include: Dune toe (red), Dune slope (green), Dune top (blue) and Building (grey).

poles (P_h* = 0.14 [-]). Further increase of pole height (P_h* = 0.83 [-]) does not influence the difference between the amplitudes, however, both amplitudes show an increase.

The subplots in figure 19 show the sedimentation patterns in the domain for varying pole height ratio (P_h*) and constant distance ratio (D*) of 1.39 [-]. For the placement of buildings on increasingly longer poles, the erosion pattern upwind of the building expands in size and stretches further underneath the building (subplots b., c. and d.). Besides, the placement of buildings on small poles (P_h* = 0.14 [-], see subplot a.) allows for the formation of a deposition region underneath the building. For medium poles (P_h* = 0.42) the deposition region underneath the building reduces in extend, whereas an area of deposition forms directly behind the building. Placing the buildings on long poles (P_h* = 0.83 [-]) results in shrinkage of the deposition region underneath the building and partly shift to erosion. Directly behind the building, increasingly more sediment deposits for increasing pole height, which explains the increase in relative deposition over the dune toe region as indicated by figure 18. The deposition tails downwind of the gap remain similar in magnitude and size for varying pole height.

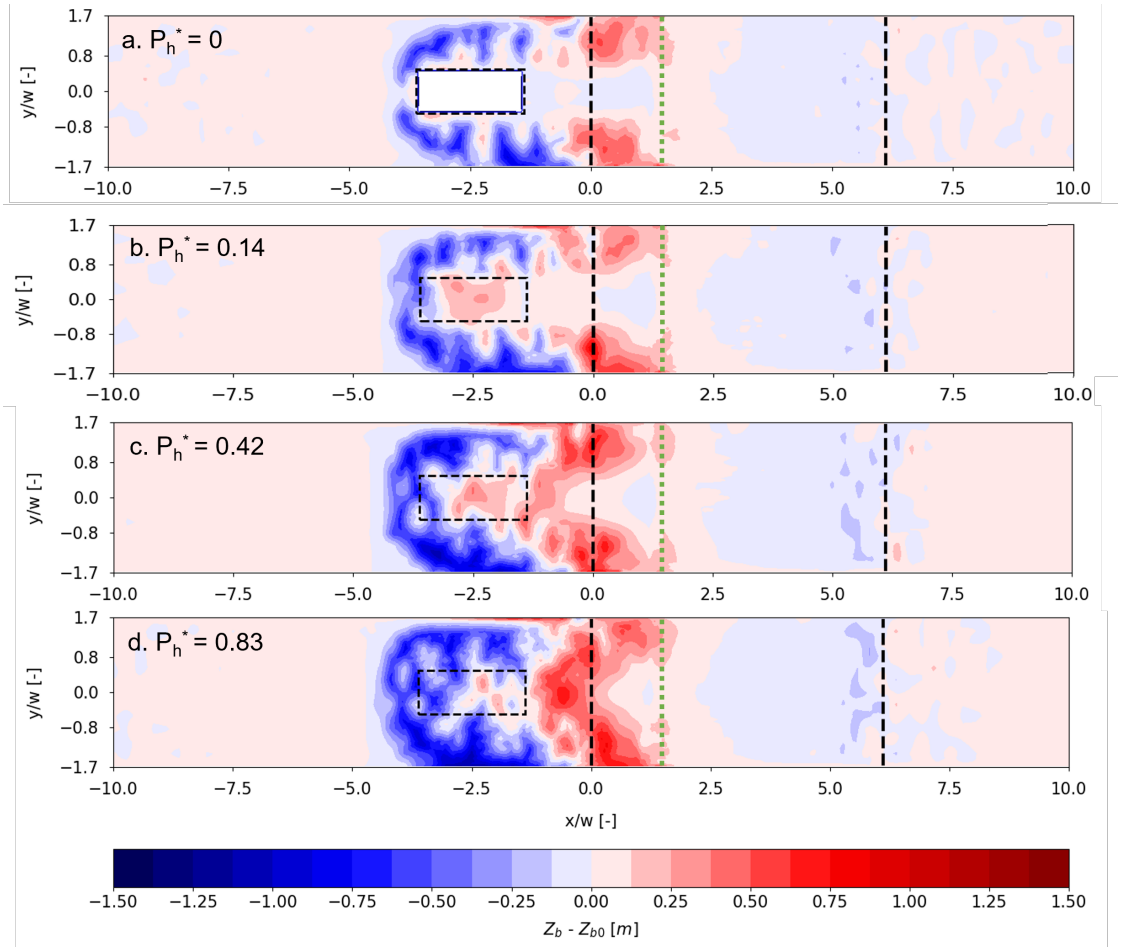

Figure 19: Sedimentation patterns (Z_b - Z_{b0}) over 24 hours for the configurations with increasing pole height ratio: a. 0; b. 0.14 ('Default building'); c. 0.42; d. 0.83 [-]. All configurations include a distance ratio of 1.39 [-].

4.4 Combined influence building-dune distance and pole height

Figure 20 shows the average relative bed level change with respect to the 'No Building' case in the four regions for all configurations as presented in chapter 3. Figure 20 a. shows increased deposition over the dune toe region for all configurations if buildings are present, whereas the magnitude depends on pole height and building-dune distance. In the region around the buildings, erosion increases for all configurations (20 d.). Over the dune slope and dune top, effects of buildings are minor independent of pole height and building-to-dune distance (20 b. and c. respectively). In general, an optimum for distance ratio (D*) in the dune toe region seems to exist, which is in the range of 0.5 - 2.5 [-] depending on pole height ratio, with maximum deposition for a distance of approximately the building width (1w) in combination with a pole height ratio of 0.83 [-]. A local maximum is found for a distance ratio of approximately 2.8 [-] in combination with a pole height ratio of approximately 0.15 [-].

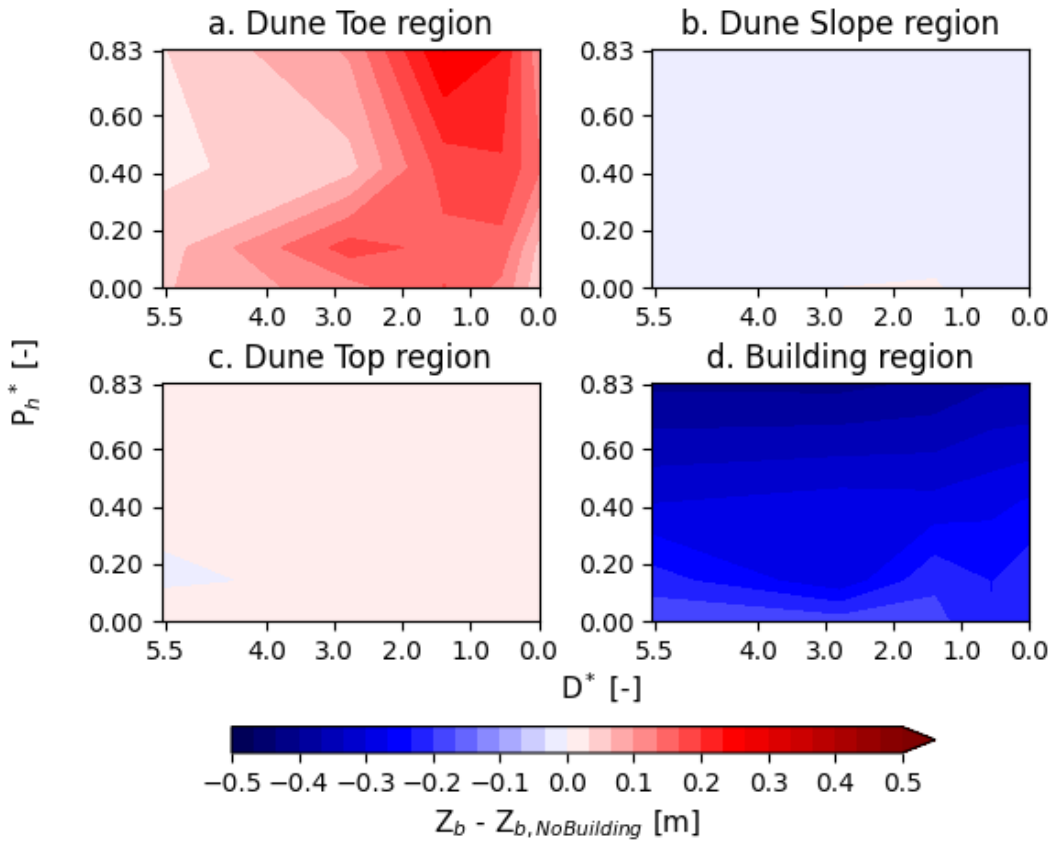

Figure 20: Influence of building-dune distance ratio (D*) and pole height ratio (P_h*) on mean bed level change relative to the 'No Building' case over 24 hours of the dune toe (a.), dune slope (b.), dune top (c.) and around the building (d.).

For the building region, increasing pole height results in enhanced erosion, whereas building-dune distance shows to have negligible influence on the strong erosion occurring around the building. The dune slope (b.) and top (c.) regions show sediment erosion and deposition respectively for almost all configurations. However, the dune slope and dune top are further analyzed based on figure 21 which includes a color bar with reduced range to show the influence of the two parameters on the dune slope and top regions on a smaller scale.

In figure 21 it can be seen that for the placement of buildings close to the dune (D* $\leq$ 3.0) the pattern for the dune slope region looks somewhat similar to that of the dune toe (figure 20 a.). In addition, erosion over the dune slope is minimum for buildings without poles (P_h* = 0 [-]) placed at a significant distance from the dune toe (D* $\geq$ 1.0 [-]). For buildings placed within a certain range from the dune (D* = 1.2 - 2.5 [-]), the erosion over the dune slope even shifts to deposition. If buildings are placed on poles (P_h* $\geq$ 0 [-]), the erosion pattern over the dune slope shows larger dependency on building-dune distance, with maximum erosion for buildings

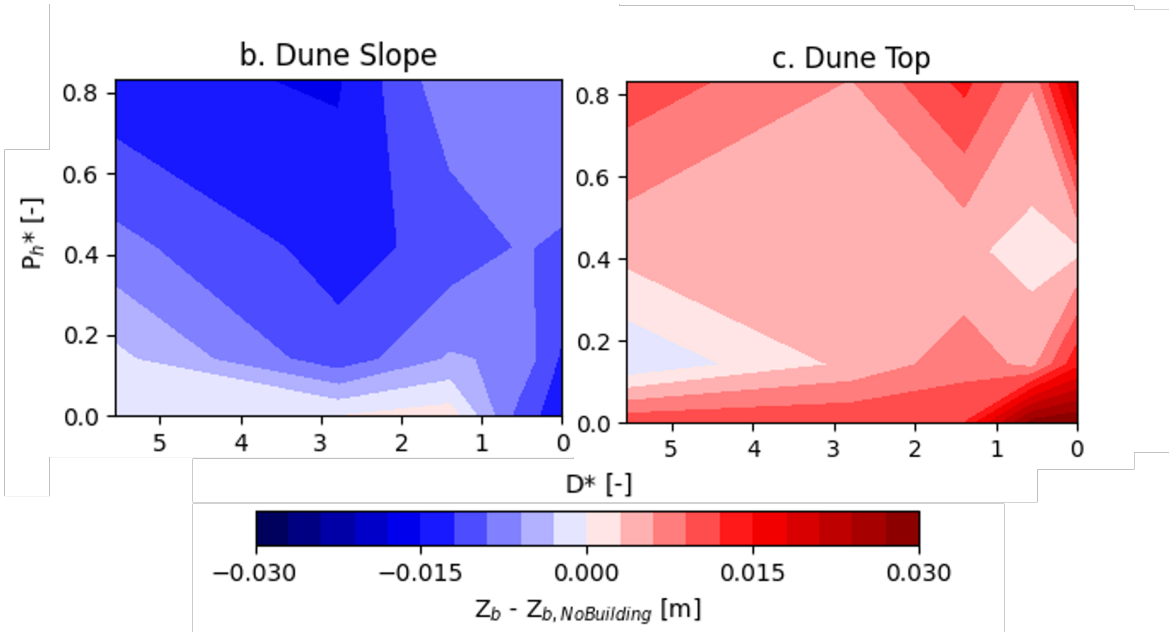

Figure 21: Influence of building-dune distance ratio (D*) and pole height ratio (P_h*) on mean bed level change relative to the 'No Building' case over 24 hours of the dune slope (b.) and dune top (c.) with adjusted color bar

placed at a distance ratio of approximately 2.8 [-]. At the dune top (c.), sedimentation patterns strongly depend on pole height and show a weaker dependency on the building-dune distance. Sedimentation over the dune top is weakest for pole height ratio ranging between 0.1 and 0.5 [-] and increases for shorter and longer poles. The sedimentation over the dune top is strongest when the row of buildings is placed directly at the dune toe (D* = 0 [-]) in combination with no poles or long poles (P_h* = 0 and 0.83 [-] respectively). Dune growth in all regions is found for buildings without poles (P_h* = 0 [-]) placed at moderate distance from the dune toe (D* = 1.2 - 2.5 [-]).

An overview of all sedimentation-erosion patterns can be found in Appendix A. In general, these figures show similar trends for pole height and building-dune distance influence as shown in sections 4.3.1 and 4.3.2. Though, if the row of buildings is placed at different distances from the dune toe, the influence of pole height alters indicating the importance of the dune shape. Figure 22 a. and b. show that for buildings placed close to the dune profile (D* $<$ 2.8 [-]), the deposition tails downwind of the gaps seem to be limited in extent by the dune profile and decrease in magnitude for placement closer to the dune (see figure 22 a. and b.). The deposition tails disappear entirely when buildings are located directly at the dune toe (see figure 22 c.). Besides, for the placement of a row of buildings at the dune toe, on long poles (P_h* = 0.83 [-]), the deposition area underneath the buildings are larger compared to placement at a certain distance from the dune (see figure 22 a., b. and c.).

As mentioned previously, figures 20 and 21 show relative growth for all dune regions when buildings without poles are placed at moderate distance from the dune (P_h =

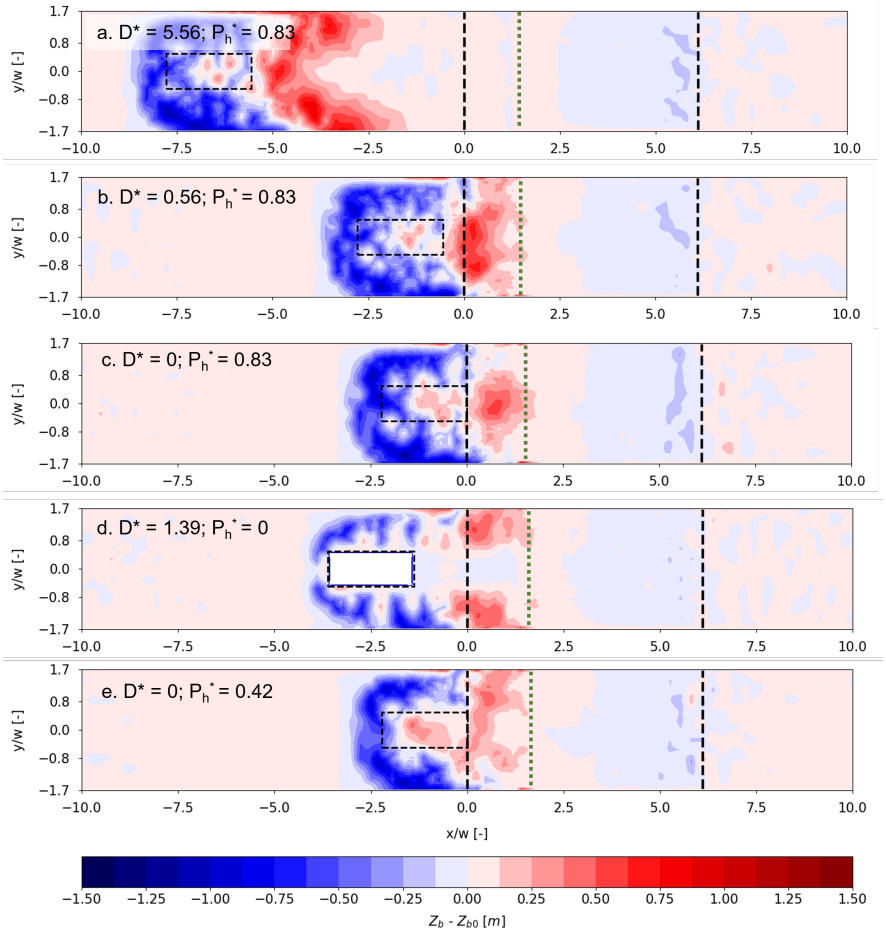

Figure 22: Sedimentation patterns (Z_b - Z_{b0}) for a selection of all configurations that contain noteworthy results over 24 hours. Configurations are shown with the following building distance ratio and pole height ratio: 5.56; 0.83 (a.), 0.56; 0.83 (b.), 0; 0.83 (c.), 1.39; 0 (d.) and 0; 0.42 (e.). The dune toe and crest are indicated by a black dashed bar over the width of the domain. A green dashed line indicates the cross-shore starting location of the vegetation.

0 and D* = 1.2 - 2.5 [-]). However, this results in large variation in bed level elevation over the width of the dune toe region, see figure 22 d. To minimize longshore variation in bed level elevation without creating areas of strong erosion over the dune profile, the row of buildings should be placed at appropriate distance from the dune (D* $>$2.8 [-], see figure 22 a.) or on poles with appropriate height (P_h* $>$0.4 [-]). For these combinations a deposition region forms directly downwind of the buildings to form similar deposition height over the width of the domain (see figure 22 b. and e.). To ensure the formation of deposition tails for buildings placed at the dune toe, pole height should be limited (D* = 0 and 0.2 $<P_h<$0.8), see figure 22 c. for no deposition tails and e. for deposition tails.

4.5 Sensitivity additional model parameters

In this chapter, the sensitivity of certain model settings is reviewed. These include vegetation, domain height, wind speed and the time between two updates of the wind field through OpenFOAM.

4.5.1 Vegetation

In figure 23, the influence of vegetation is visualized. Vegetation has been included as a reduction of bed shear stress with a factor of approximately 2 caused by a vegetation cover of 20%. The decision for this 20% cover is somewhat arbitrary, though a rough estimation allowed to include vegetation in the model results as is present in the field. The comparison can be found in figure 23. The influence is mainly visible over the dune slope and dune top, where vegetation is implemented. Around the building and over the dune toe, differences are minor. Over the dune slope, exactly from the start of the vegetation, and even more at the crest, the erosion is reduced significantly. Besides, over the dune top, erosion may even be shifted to deposition in the presence of vegetation. When no vegetation is present, the variation between the minimum and maximum amplitudes is significant. In general, effects of vegetation are significant and reduce erosion over the vegetated area. However, minor over- or underestimation of vegetation effects could largely exacerbate or alleviate final results, indicating the importance of appropriate vegetation settings.

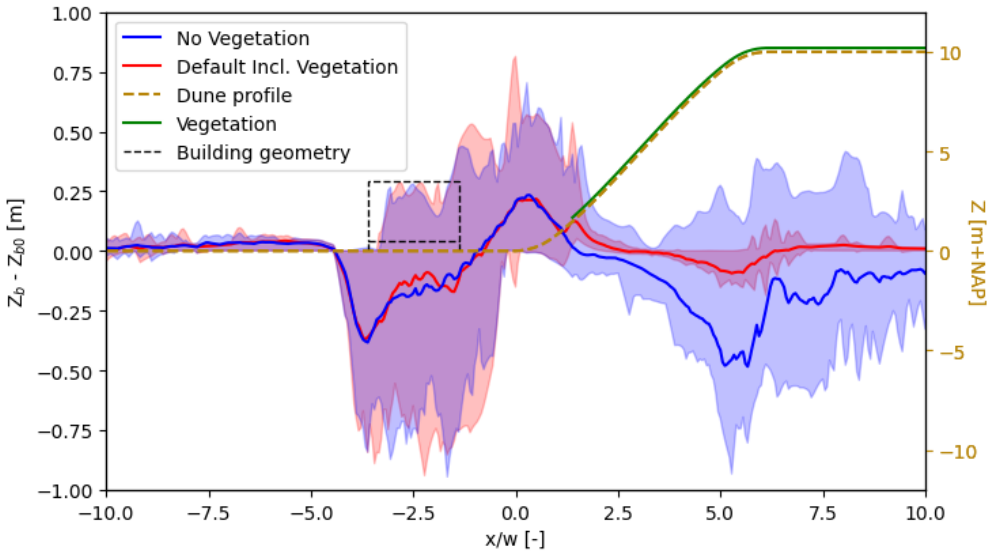

Figure 23: Average bed level change and minimum and maximum amplitudes over the width of the domain for the 'No Vegetation' and 'Default' cases over 24 hours. The building geometry, dune profile and the location of vegetation are included in the figure

4.5.2 Domain Height

All configurations have been run for a domain height of 40m, but since the bed level elevation of the beach is different from that of the dune, the vertical spacing for the wind decreases from 40 meters over the beach to 30 meters over the dune. However, the wind field is constrained by the continuity which states that the same volume of air that enters the domain through the inlet should exit the domain through the outlet. This causes compression and as a result an increase in wind velocity over the dune with a factor of approximately 40/30 = 1.33. To get better understanding of the influence of this factor, the domain height is increased to 80 meters, which corresponds to 70 meters between the dune top and the domain height. As a result, wind velocity increases with a factor of approximately 80/70 = 1.14. The effect of the increase of domain height from 40 to 80 meters can be seen in figure 24. Mainly at the dune crest, less sediment erodes. Variation between the minimum and maximum amplitudes is similar for both cases. Besides, just downwind of the building, an increase in deposition can be found. The effects are small, though are not negligible.

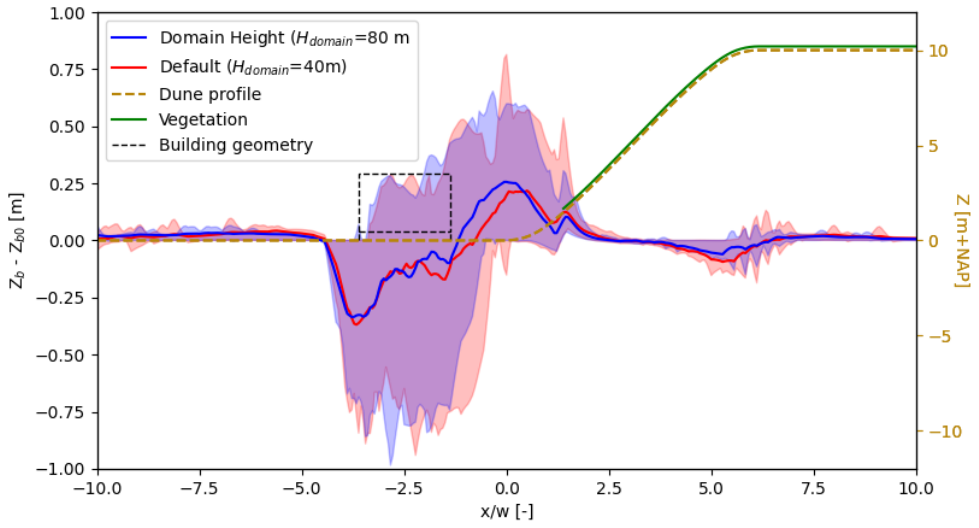

Figure 24: Average bed level change and minimum and maximum amplitudes over the width of the domain for the 'Domain Height' and 'Default' cases over 24 hours. The 'Domain Height 80 m' case includes the top boundary at a height of 80 meters, whereas the 'Default Building' case contains the top boundary at 40 meters. The building geometry, dune profile and the location of vegetation are included in the figure

4.5.3 Wind Speed

A wind speed of 17 m/s is used in the simulations to speed up the morphodynamic process. However, this wind speed is considered to be a storm and model results do not represent morphological development for milder wind velocity. Therefore, the model is run with a lower wind speed of 10 m/s to get insight into the influence

of milder wind speed on morphological bed evolution and to see whether similar sedimentation patterns occur. Figure 25 shows that similar sedimentation-erosion patterns form for a configuration with lower wind speed. However, the mean sedimentation patterns are much smaller in magnitude as well as the difference in amplitudes.

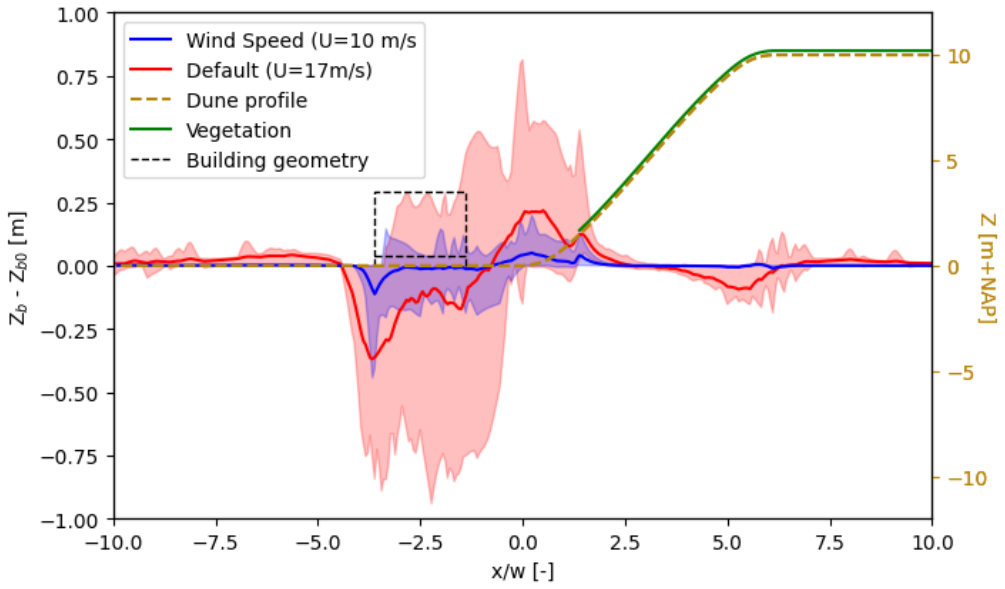

Figure 25: Average bed level change and minimum and maximum amplitudes over the width of the domain for the 'Wind Speed' and 'Default Building' cases over 24 hours. The 'Wind Speed' case includes a reference wind speed of 10 m/s and the 'Default' case 17 m/s. The building geometry, dune profile and the location of vegetation are included in the figure.

4.5.4 Time between wind field updates

The coupling model relies strongly on the number of wind field updates through OpenFOAM. Higher resolution results are created for a smaller time step between wind field updates, though increase computational cost. The decision for 6 wind field updates over a period of 24 hours (4 simulation hours between updates) is somewhat arbitrary and has not been well investigated. Therefore, simulations are performed for the 'Default Building' case with 2 and 8 hours between two wind field updates through OpenFOAM. Results are shown in figure 26. It can clearly be seen that for an increase in number of updates (shorter time step) erosion underneath the building decreases whereas the bed level at the start of the vegetation increases. The increase in bed level height at the start of the vegetation is not visible the 'OF 8 hour' run. The difference between the minimum and maximum amplitudes remains similar as well as the sedimentation pattern over the dune top.

The subplots in figure 27 show the sedimentation patterns for a time step between

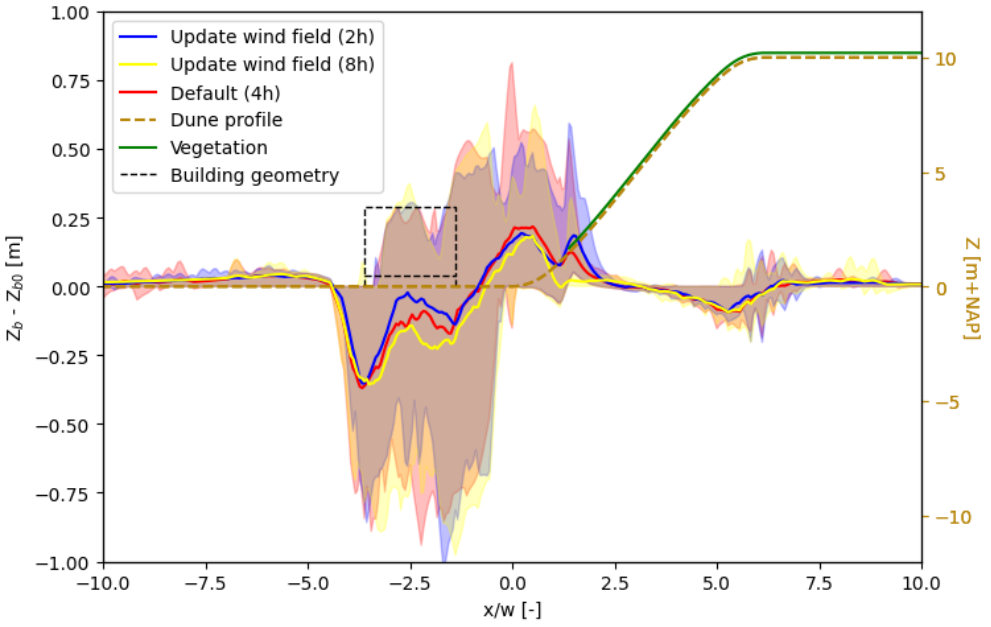

Figure 26: Average bed level change and minimum and maximum amplitudes over the width of the domain for the 'Update wind field 2h', 'Update wind field 8h' and 'Default (4h)' cases over 24 hours. The time between two updates of the wind field through OpenFOAM are included in the case names. The building geometry, dune profile and the location of vegetation are included in the figure.

two updates of the wind field of 2 hours, 4 hours ('Default') and 8 hours respectively. A large difference can be found in the patterns of increasing and decreasing the time step compared to the 'Default (4h)' case. Increasing the time step from 4 hours to 8 hours shows large effects on the erosion pattern around the building and the deposition tails downwind of the gaps. The erosion pattern is rather uniform, without the formation of humps (see figure 27 a.) whereas the deposition tails decrease in extent. This indicates the importance of increasing wind field update frequency by reducing the time step between two wind field updates from 8 to 4 hours. However, decreasing this time step further, from 4 hours to 2 hours, seems to reduce the erosion around the building even further. In addition, reducing the time step from 4 to 2 hours shows deposition tails to extend further onto the dune. This indicates that an increase in amount of wind field updates results in larger variation in height of sedimentation-erosion patterns around the buildings and further extension of the deposition tails onto the dune.

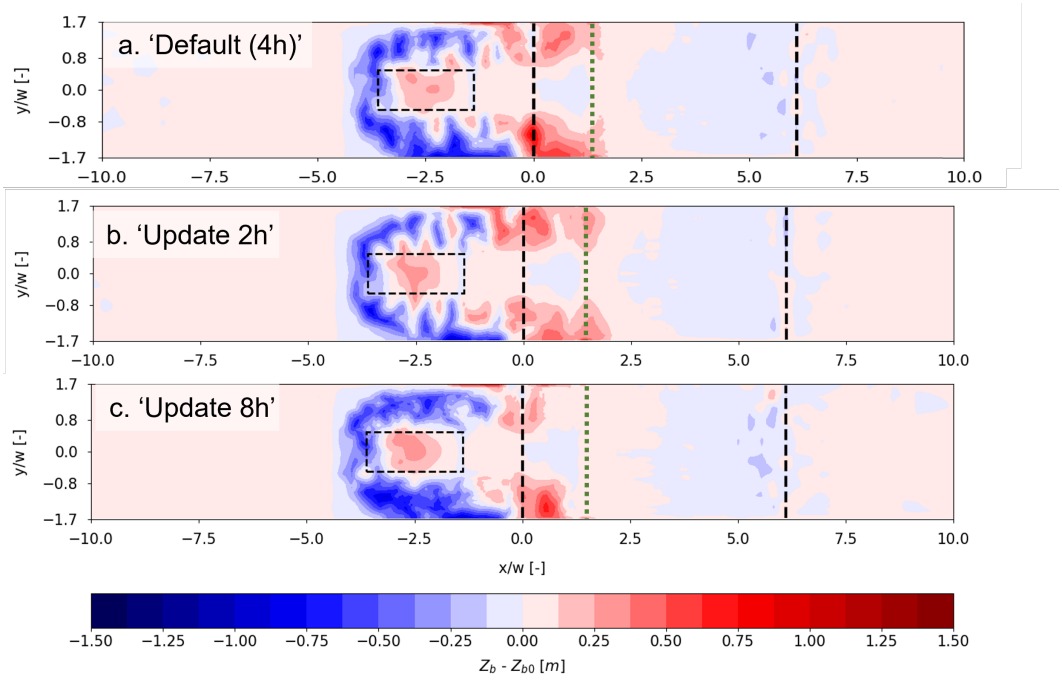

Figure 27: Average bed level change and minimum and maximum amplitudes over the width of the domain for the 'Update wind field 2h', 'Update wind field 8h' and 'Default (4h)' cases over 24 hours. The time between two updates of the wind field through OpenFOAM are included in the case names. The building geometry, dune profile and the location of vegetation are included in the figure.

5. Discussion

In this chapter, the results from chapter 4 are discussed as well as the performance of the model. Afterwards, limitations to the study are discussed followed by a validation of the model with field data.

5.1 Bed morphodynamics around a dune profile downwind of a row of buildings on poles

Within this section, the results are discussed in different parts. At first, the sedimentation patterns that occur as a result of a dune shape are discussed. Next, the influence of a row of buildings on bed morphology in the domain is compared with literature. At last, the results on the influence of building-dune distance and pole height are interpreted.

5.1.1 Sedimentation patterns induced by a dune shape

Sedimentation patterns that form due to the shape of a dune agree to findings by other studies [50] [18] and correspond to expectations based on wind field patterns [34] [35] [14] [17]. Besides, the sedimentation patterns are in the same order of magnitude, which validates the use of this model for simulating morphological bed evolution over a dune profile. The shape of the dune profile causes wind deceleration upwind of the dune and over the dune toe, whereas velocity strongly increases towards the dune crest [34], [35] [18]. As a result, sediment deposition is found over a large region upwind of the dune and partly over the dune toe, whereas erosion is found over the dune crest, see figure 14. Jonkheer [18] found deposition height over the dune toe region. This difference can be explained by the reduction in entrained sediment concentration, as included in AeoLiS, towards the dune toe due to deposition upwind of the region, which was not included in the study by Jonkheer [18]. In addition, Jonkheer [18] found cross-shore variation in deposition and erosion just downwind of the dune crest, which was also observed in our findings.

5.1.2 Sedimentation patterns induced by a row of buildings with varying pole height and building-dune distance

It may be expected that buildings trap sediment and block aeolian sediment transport in duneward direction affecting dune growth [51] [9] [15]. However, the results of this study contradict this and agree with the statement that buildings could enhance dune growth, since dune growth over all regions was found for buildings without

poles at moderate distance from the dune toe ($1.2 < D^* < 2.5$ [-]), see figures 20 and 21 [14] [3] [16] [1].

With the introduction of a row of buildings on poles (D^* = 1.39 [-] and $P_h{}^*$ = 0.14 [-]) upwind of the dune profile, new insights are created on changes to dune morphology induced by a row of buildings on poles. The sedimentation over the dune toe (see figure 14) originates from the eroded area around the building, caused by flow acceleration around the building and funneling effects between neighbouring buildings [13] [62] [3] [15] [16] [1]. Due to flow expansion downwind of the gaps, flow decelerates and as a result, deposition tails form. Also, sediment deposits underneath the building, which can be explained with similar reasoning, compression of airflow between the poles and expansion downwind of the buildings underneath the building [1]. The sedimentation pattern over the width of the domain was expected to be symmetrical. According to figure 13 this is somewhat true, though there are minor differences. These might be caused by inconsistencies in the wind field as computed by OpenFOAM. Due to the repeating interaction between the wind field and bed, these small variations may grow over time. Additionally, it was found that placing buildings on poles ($P_h{}^* > 0$ [-]) does not necessarily minimize erosion or enhance deposition over all regions of the dune as indicated in previous studies [25] [1]. Namely, our findings indicate that the sedimentation patterns are also dependent on the distance at which the row of buildings is placed.

The sedimentation patterns in the vicinity of the building generally agree with findings by previous research on beach buildings on poles [15] [16] [1]. This validates the use of this model setup including cyclic boundary conditions to represent a row of buildings for the computation of morphological bed evolution around a row of buildings on poles. However, differences are found in the placement of buildings without poles in relation to the placement on poles. The field experiments by Poppema [15] showed that the placement of buildings on small poles ($P_h{}^*$ = 0.2 [-]) causes a region with strong deposition to form downwind of the building, which seems to be located underneath the building in our results, see figures17. Besides, Poppema [15] found that the deposition tails decrease in magnitude and increase in length for increasing pole height, while our results indicate the opposite. The difference could be explained by the varying wind conditions that were present during the field experiments, whereas the model includes one wind direction. Varying wind direction may flatten patterns, whereas constant wind direction may promote further formation of the patterns.

Additionally, sedimentation-erosion pattern in the surrounding of the building on long poles ($P_h{}^*$ = 0.83 [-]) located far from the dune (D^* 5.56 [-]) corresponds to findings by Pourteimouri et al. [1]. However, a difference is found in the formation of the deposition tails downwind of the gaps. According to Pourteimouri et al. [1] the deposition tails are located further downwind and become longer in extent for the placement of buildings on poles ($P_h{}^*$ = 1 [-]) compared to no poles, which is in agreement with

Poppema [15]. Our results show that the deposition tails remain in place and do not stretch over longer area but increase height. This difference could be related to the influence of the dune shape on sedimentation patterns compared to a flat bed, which causes flow deceleration upwind of and over the dune toe. Since erosion upwind and around the building increases for longer poles due to flow compression [1], more sediment gets suspended, which may transport further since the flow deceleration zone is located higher. However, due to the presence of a dune profile, wind velocity between the dune and row of buildings is reduced, which promotes deposition between the buildings and dune profile. As a result, the length of the area over which deposition occurs is limited as well as the sediment transport in downwind direction. Another reason could be related to the difference in gap width ratio (g* = s/(s+w)) which defines a parameter to define relation between gap spacing of two neighbouring buildings (s) and building width (w). Pourteimouri et al. [1] used a gap width ratio of 0.5 [-], which is similar to the ratio that was found to create strongest funneling effects. The funneling effects cause strong wind acceleration through the gap and just downwind of the gap causing sediment to be transported with higher velocity further downwind of the gaps. In our study, a gap width ratio of 8.4/(8.4+3.6) = 0.7 [-] is used, which is slightly larger than a defined critical gap width ratio (g* = 0.67 [-]) beyond which funneling effects are found to be minimal and wind fields of two neighbouring buildings hardly showed interaction [15] [1]. As a result, sediment travel with lower velocity through the building's gaps and deposit closer to the building gaps.

In agreement with studies by Poppema [15] and Pourteimouri et al. [1], results show that increasing pole height enlarges erosion underneath the front face of the buildings. As a result, the deposition region underneath the buildings grows up to a critical pole height ratio (P_h* = 0.1 - 0.4 [-], see figure 19) after which it declines. This may explain the strong increase in downwind sediment transport found by Pourteimouri et al. [1] for increasing pole height ratio from approximately 0.3 to 0.8 [-]. As a result of a reduction in deposition, more sediment travels to the flow deceleration zone downwind of the building, allowing a sediment deposition area to form. New insights are found in the results related to the influence of gap width ratio. Namely, the patterns seem to become wider for increasing pole height, which indicates that the findings by Qian et al. [34] [35] and Poppema [15] on gap ratio does not hold for structures on poles.

New insights are found downwind of the buildings if placed close to the dune toe (D* $\leq$ 2.8 [-]). Deposition tails were found to be limited in extent by the dune. In addition, placing buildings closer to the dune reduces the height of the deposition tails, which fully disappear if located directly at the dune toe. The stretch of the deposition tails seems to be limited by the presence of vegetation, which contradicts the expectation that vegetation would promote deposition [49] [12] [50] [18]. A potential explanation can be related to the avalanche process included in AeoLiS which limits the potential increase in bed level to 4°, considering an initial bed slope over the

dune of 30°. Another explanation for the reduction in magnitude and disappearance of the deposition tails could be related to the wind fields around the building geometry and over the dune shape. The dune shape causes flow acceleration over the dune slope and maximum velocity at the dune crest [34] [18]. For increasing pole height, the flow deceleration zone downwind of the building gaps is elevated higher and therefore interferes stronger with the flow acceleration zone of the dune shape. As a result, the wind velocity downwind of the gaps decelerates less, resulting in less to no deposition downwind of the gaps onto the dune profile.

Poppema [15] established a linear relation of the height (H) and width (W) of the wind-facing wall of the buildings with the horizontal extend of the deposition tails ($B = H^{2/3}W^{1/3}$). In our study, the results are scaled with the building width only, which equals the width of the wind-facing wall due to the wind forcing perpendicular to the front face of the building. However, the relation that has been proposed by Poppema [15] is based on field observations around buildings placed on the bed and it is unknown whether the relation holds for buildings on poles, as is included in our study. In addition, the building geometry and wind incidence angle have not been varied throughout this study. Therefore, the wind-facing wall was constant and results can easily be re-scaled with other building parameters.

In addition, results highlight the importance of vegetation which corresponds to findings of other researchers [49] [12] [50] [18]. The presence of vegetation highly affects sediment transport over the dune slope and top and as a result, only small changes in relative bed level change are observed over the dune slope and dune top.

5.2 Limitations

In this section, multiple aspects of this study are discussed that can be improved to create more reliable and relevant results. This chapter discusses limitations in the usage of the numerical coupling model, the model setup and the limitations in the computation of aeolian sediment transport.

5.2.1 Numerical model

This study makes use of a coupling model as proposed by Pourteimouri et al. [1]. The coupling combines an airflow model in OpenFOAM with the sediment transport model AeoLiS [19]. For the coupling settings and both models, decisions had to be made regarding model settings. Two model settings were altered to see the influence on model output, see sections 4.5.2 and 4.5.4. Regarding the time step between two updates of the wind field, it was found that the sedimentation-erosion patterns that form differ in certain regions. The sedimentation-erosion patterns showed that the current model setup did not fully allow to capture the erosion pattern around the building and the extent of the deposition tails onto the dune correctly. However, these differences are limited to small areas within the domain. Multiple other model

settings for AeoLiS and OpenFOAM should be tested in order to improve the reliability of the model and potentially reduce computation time without reducing the model's accuracy. In addition, Jonkheer [18] indicated high sensitivity of the roughness height parameter in the computation of the wind field. Jonkheer [18] found that an increase in roughness length with a factor of 3 increases bed shear stress with a factor of approximately 1.4 at the dune crest and less over other parts of the domain. Increasing the roughness length could increase the bed shear stress and induce more sediment transport. As a result, a reduced quantity of sediment deposits over the dune toe and sediment erosion is increased, especially over the dune crest, which may increase deposition over the dune top.

5.2.2 Model setup

In the setup of the model, various choices have been made related to the dune geometry, building geometry and domain dimensions to simulate similar conditions. These choices might cause large differences between the model and field conditions resulting in significant differences in patterns or trends. Important differences to reality are:

- The building geometry is based on the row of beach buildings as are placed on the Zuiderstrand near Kijkduin [54]. These buildings are included in the model simplified as a cuboid shape. Besides, in reality, stairs are placed upwind of the building, which could have large effect on sedimentation patterns by trapping sediment or altering the wind field in the vicinity and underneath the building. Besides, Nordstrom et al. [9] indicated the importance of building material, which influences the airflow pattern around the building. For improved inclusion of building geometry, the full design of the building should be included in more detail.
- The dune is designed as 10 meters high with a flat top. No longshore variation was implemented over the dune profile. However, in reality, dunes may form with much spatial variation in longshore direction over dune profiles [63]. In addition, dune shape interacts with the wind field and the effects on dune morphology might be highly influenced by the shape of a dune.
- A large difference with reality can be found in the implementation of the wind characteristics. The model includes constant wind forcing at the inlet with high wind speed that may be considered as storm wind speed and constant incidence wind angle. In reality, wind continuously varies in speed and direction [55]. The high wind speed could cause irregular flow conditions in the domain with requires further research. Besides, sediment transport in duneward direction was found to be significantly enhanced for larger wind angles [16]. As a result, the computed morphological bed evolution downwind of the buildings could become significantly higher for oblique wind angles.
- At last a flat beach is used, whereas in reality, the beach is sloping. However,

the effects on an inclined bed on sediment transport towards the building and dune profile are unknown and could provide better insight into the influence of beach slope.

5.2.3 Sediment transport

This study includes a simplified form of vegetation over the dune shape, namely as a reduction in bed shear stress. The bed shear stress as computed by OpenFOAM is exported to AeoLiS which modifies the bed shear stress. Though, since the influence of vegetation is included only after the wind field is computed, the airflow acceleration above the canopy is not included in the wind field [49]. Additionally, the vegetation root system stabilizes the bed allowing bed slopes beyond the angle of repose that has been used in our study (34°) [12]. Since this study simulated change of bed level elevation over a period of 24 hours, vegetation growth was not considered. However, in reality, buildings are often placed for multiple months, such as for the beach buildings near Kijkduin [54], in which vegetation dynamics might become important for further development of the dune profile.

In addition, other bed surface properties as present on the beach may limit aeolian sediment transport. Grain sorting has not been considered, whereas over time this may lead to reduced aeolian sediment transport due to the formation of beach armoring [64]. Additionally, moisture content of the bed significantly controls release of particles for aeolian sediment transport [65]. Rainfall and tides increase moisture content and velocity threshold of particles, whereas the drying process creates a thin layer of dry sand on the surface which can be set to motion more easily. The exposed layer may erode after which a deeper layer gets exposed to the drying process. Moisture content has not been included in our study as the bed is assumed to consist of a thick layer of dry sediment. However, on the beach, this sediment transport may be much smaller in magnitude since the drying process limits the rate at which sand may erode. Including this drying process in a simplified form may already give better insight into the actual magnitude of sediment transport on a beach. Additionally, fetch length is the length over which wind flow may set sediment particles to motion. This is considered to have no limiting effect in our study due to the long upwind beach length (47 meters) in wind direction, see Appendix E. However, this has not been studied and might affect patterns, especially for large distance ratio configurations since the particle concentration did not reach its full capacity yet.

At last, this study simulated aeolian sediment transport over a period of 24 hours directly after the buildings are placed on the beach. The wind field over the flat beach and dune profile experiences an extreme change as a result of the placement of a row of beach buildings. The alteration of the bed as a result of this extreme change in wind field is strongest in the short period directly after the buildings are placed. Therefore, the magnitude of the sedimentation patterns that are observed in this study may not fully represent long-term evolution (seasonal) of the bed in the vicinity of a row of buildings and dune profile.

5.3 Validation with Kijkduin beach buildings

To get better insight into the performance of the model with respect to simulation bed morphology around a row of buildings on poles upwind of a dune profile, the model results are compared to field data of the beach buildings at Kijkduin. The 'Default building' case represents the model results for the Kijkduin beach buildings case, with similar building dimensions, pole height and distance to the dune foot during the placement of the buildings. Data has been collected on the 10th of July 2017 and on the 9th of October 2018, whereas in both years the buildings were placed on the 1st of March, see figure 12.

First of all, the formation of sedimentation patterns is closely linked to wind direction. At Kijkduin the dominant wind direction, thus the main driver for the formation of sedimentation patterns, is Western, whereas the front face of the beach buildings points in Northwestern direction at an angle of 45 $^{\circ}$ with respect to the dominant wind direction. This differs from the wind direction in our study due to which a one-to-one comparison cannot be made regarding the sedimentation patterns in the surrounding of the pattern. However, the sedimentation patterns can still be compared roughly in terms of magnitude and pattern formation with respect to the dominant wind angle. Thus, sedimentation patterns of figures 12 and 13 b. are compared with respect to wind dominant wind angle.

Sedimentation patterns that are found in field surveys and in our results are roughly in the same order of magnitude, 10^{-1} m. The erosion patterns that form are approximately 0.2 m lower whereas deposition over the dune toe is approximately 0.2 to 0.4 m (compared to year 2017 and 2018 data respectively) higher. Though, the patterns that were found at the Zuiderstrand have been created by aeolian sediment transport over a time period of approximately 4.5 months, whereas our results formed after 1 day of simulation. This difference in morphological development rate could be related to the high wind speed in the domain, which results in a significantly higher erosion and deposition rate in the model. In reality, wind speeds of 17 m/s are rare events and are mainly measured over the winter period [55], during which buildings are not present on the beach. Besides, the wind incidence angle varies over time causing an overlap of various sedimentation patterns, flattening out sedimentation-erosion patterns. Additionally, the model includes an abundant of dry sediment, whereas at the beach various supply limiting processes are present. This could explain the deeper erosion pattern and higher sediment depostion over the dune toe. Besides, the magnitude and patterns around the buildings are similar in the data that was are observed in October 2018, which formed over a period of 3 months longer with respect to the data that was observed in July 2017. This indicates an equilibrium for the sedimentation-erosion at the upwind side of the buildings, which could be reached much earlier after the placement of beach houses on the beach than indicated by the data. To conclude, the model overestimates the sedimentation rate. However, the patterns that are simulated are in the same order of magnitude

as observed in field data on seasonal time scale.

Additionally, similar sedimentation patterns can be found. Considering the alignment of the dominant wind direction, both figures 12 and 13 b. show similar patterns. However, a large difference can be found at the upwind side (or corner in figure 12) of the building. Note that the survey data includes a path of concrete slabs in front of the buildings. The survey data of both years shows erosion in front of the wind-facing section of the building, which is in line with the results shown in this study. Though, upwind of the front face of the building, deposition can be found which stretches in upwind direction. This can be explained by the presence of stairs at this side of the building in combination with deposition upwind of the buildings. Sand may be deposited by the owners of the buildings to remain a small elevation difference between the stairs and the bed. This deposition pattern might be shaped by the dominant wind angle in combination with upwind deposition to form the oblique deposition pattern that is observed.

Something interesting can be found in the data of the year 2018, which has been observed approximately 3 months after the bed elevation of the year 2017. Namely, the dune profile has significantly extended in between the buildings. This pattern can also be observed in figure 13 b. It does not become clear whether the building enhances dune growth in the gaps and whether dune growth is reduced downwind of the building. Nevertheless, it can be concluded that the survey data and our model results agree that this specific row of buildings configuration causes strong longshore variation in bed level elevation over the dune profile for a row of buildings on small poles (P_h* = 0.14 [-]) at moderate distance from the dune (D* = 1.39 [-]).

This validation provides insight into the patterns that form over long-term seasonal presence of a row of beach buildings on poles in front of a coastal dune. This validation did provide that the patterns that are simulated by the model represent patterns that form on a small-time scale. However, the patterns that are observed in the seasonal time period do comply with the patterns that have been simulated by the model. The data does provide that the dune extends whereas the sedimentation-erosion patterns around the front section of the building remain similar in magnitude, indicating an equilibrium for the magnitude of these patterns. This could be reached within a significant shorter time period than the time period between the placement of the buildings and the surveys.

6. Conclusions and recommendations

This chapter consists of two sections. First, the conclusions are presented which provide answers to the research questions. Next, a section is dedicated to the recommendations for future studies.

6.1 Conclusions

This study has been performed using a coupling model between a 3D airflow model in OpenFOAM and the 2DH aeolian sediment transport model, AeoLiS [19]. Various model runs have been performed with a dune profile and different building configurations. The building configurations included variation in pole height and building-dune distance. The results were computed using a coupling model between OpenFOAM and AeoLiS. The two research questions of this study are addressed below. The first research question is stated as follows:

1. How is bed morphology altered over a vegetated dune profile with the placement of a row of buildings on poles at the beach-dune interface?

First of all, the shape of a dune with smooth edges causes flow deceleration upwind of the dune toe and over the dune. With the occurrence of aeolian sediment transport, this flow deceleration zone induces sediment deposition upwind and partly over the dune toe. Over the dune slope, flow accelerates, resulting in erosion of sediments. Just downwind of the dune crest, deposition and erosion may occur due to variation in flow velocity.

With the placement of a row of buildings on poles in front of a dune profile, sedimentation-erosion patterns are significantly altered over different sections of the dune profile. More sediment is deposited in the lower section of the dune, whereas enhanced erosion occurs at the dune crest. Over the dune slope and the dune top, the magnitude of sedimentation patterns is substantially smaller compared to the patterns over the dune toe. This is related to the presence of vegetation, which stabilizes the bed by reducing bed shear stress, indicating the importance of vegetation for the formation of dunes. As a result erosion over the dune slope is significantly reduced and deposition may even occur at the dune top. The shape of the buildings and funneling effects through the building gaps cause strong erosion directly in front of the buildings and through the side gaps. The entrained sediment is deposited in the form of deposition tails downwind of the side gaps or underneath the building due to the presence of flow deceleration zones.

The second research question is stated below:

2. How do varying building pole height and building-dune distance of a row of beach buildings in the beach-dune interface influence bed morphology over a vegetated coastal dune?

The sedimentation patterns over various regions of the dune showed dependency on both the pole height and building-to-dune distance. The results indicated that dune growth may be enhanced by the placement of a row of buildings with an appropriate choice of pole height and building-dune distance. The results showed that the maximum amount of sand deposits in the dune for buildings at a distance of 1 times the building width on long poles (P_h* = 0.8), with most deposition over the dune toe and minor erosion over the dune slope. Overall growth for all dune regions was found for a row of buildings without poles (P_h* = 0 [-]) placed at moderate distance from the dune (D* = 1.2 - 2.5 [-]). However, this combination results in significant longshore variation in bed level elevation over the dune toe, which might be considered undesirable. To minimize longshore variation without creating areas of strong erosion over the dune profile, it is recommended to place the row of buildings at appropriate distance from the dune toe (D* $>$2.8) or on sufficiently long poles (P_h* $>$0.4 [-]). In addition, for the placement of the buildings at the dune toe, it was found that pole height should be limited (0.2 $<P_h$* $<$0.8).

For an increase in building pole height, erosion patterns around the buildings and deposition downwind of the buildings become larger in magnitude. Underneath the building, a deposition region forms due to local wind deceleration downwind of the poles. If poles are sufficiently high (P_h* $\geq$ 0.4 [-]), the effects of flow acceleration and deceleration by the poles seem to become less important, which allows part of the sediment to be transported downwind. This suspended sediment is transported directly behind the building and settles to form deposition due to the flow deceleration zone located downwind of the building. However, if the row of buildings is placed sufficiently close to the dune profile (D* $\leq$ 2.8 [-]), the deposition tails are limited in extent. For elevating the buildings on higher poles, the deposition tails decrease in magnitude and may even fully disappear (P_h* $\geq$ 0.8 [-]), due to interaction between the building-induced flow deceleration zone and the dune-induced flow acceleration zone.

If buildings are placed further upwind of the dune toe (D* $\geq$ 4.0 [-]), the influence of the row of buildings on dune morphology seems to become minimal, since the altered wind field downwind of the building does not stretch onto the dune profile.

In addition, the elevation of a row of buildings on poles, provides new insights into the effects of gap width of funneling effects. Namely, the wind fields around individual buildings seem to become wider for increasing pole height, due to which the critical gap width for interaction between the wind fields of two neighbouring buildings becomes lowers.

When placing a row of buildings in front of a vegetated coastal dune with minimal impact on bed level change and variation around the building for usability purposes, it is recommended to place the buildings on the bed. However, this may result in strong longshore bed level elevation difference downwind of the row of buildings, thus should be considered thoroughly.

6.2 Recommendations

This is the final section of this report and provide recommendations to improve further research into this topic:

- Based on the results of this research on the placement of a row of cuboid buildings with a specific geometry and significant gap width on the beach upwind of a vegetation coastal dune, it is recommended to place the row of buildings without poles at moderate distance (approximately 1.2 to 2.5 times the building width) to enhance dune growth over all sections of the dune profile without considering longshore bed level variability. To minimize longshore variation, buildings should be placed at substantial distance (D* $>$4 [-]) or on poles of sufficient length (P_h* $>$0.4). As the row of buildings is placed at the dune, longshore variation can be minimized by placing the building on poles of limited height (0.2 $<$$P_h$* $<$0.8). However, this study did not include vegetation growth and varying wind conditions. Besides, the sedimentation-erosion patterns for a row of buildings on poles may vary for different building height and building length (and form a relation as found by Poppema [15] for buildings without poles) as well as gap width ratio between neighbouring buildings.
- To improve the ability of the model to simulate real-world morphological patterns, cyclic boundary conditions in AeoLiS should be implemented appropriately for wind directions other than the alignment of the grid cells. In this way, varying wind direction can be included in the model together with varying wind velocity to include varying wind conditions based on historic data. Due to the high computational cost, multiple short-term model runs with varying wind conditions can be combined to get insight into the long-term morphological bed level evolution. With respect to the wind data observed at Kijkduin [55], a model run can be performed with strongest wind speed (17 m/s) at an angle of 45° (West) and systematically reducing wind velocity to 8 m/s (threshold wind speed for aeolian transport) for varying angles towards -90° (North-East) and 120° (South). With respect to the Kijkduin case, the occurrence of sufficient wind speed (U $>$8 m/s) for aeolian sediment transport is observed for wind directions ranging from -120 to 120 degrees with respect to the building orientation [55]. The strong winds prevailing originate from the Western direction.
- The coupling settings used in this study made use of a wind field update every 4 hours. However, a sensitivity analysis in which the time step varied showed that there is significant difference in morphological bed evolution over a period

of 24 hours when the resolution of the wind field updates is further increased from 4 hours to 2 hours. For that reason, it is recommended to reduce the time step between two wind field updates in future research at least to once every 2 hours. However, the variation in the time step was limited and further reduction in the time step significantly improves the precision of the calculations. However, increasing the number of wind field updates becomes more computationally expensive. Therefore, further research is recommended into the time step between two wind field updates to determine the number of wind field updates. However, it is recommended to reduce the time step from 4 hours to 2 hours if the computational power allows it.

- In this study, a simplified form of vegetation is included. In the results, it is visible that the influence of vegetation is significant and this is in agreement with other studies. However, the magnitude of the reduction in bed shear stress induced by the vegetation over the dune slope and top has not been researched and requires more investigation to improve the reliability. In addition, the influence of vegetation on the wind field can be incorporated in the airflow model in OpenFOAM to account for flow alterations as a result of vegetation characteristics contrary to the alteration of the bed shear stress by AeoLiS. Besides, for the investigation of long-term bed level evolution over the dune profile, vegetation growth is required to be included in cross-direction to allow dune expansion as was found in the field survey over the Zuiderstrand near Kijkduin on the 9th of October 2018.
- In a future study, it is recommended to revise the method that is used to define the dune regions. Namely, it was found that the magnitude of erosion over the curvature of the dune slope did become clear from the regional relative mean bed level change since the dune slope region was highly influenced by the presence of deposition tails at the lower part of the dune slope. To get better insight into the effects of a row of buildings and varying building characteristics on dune morphology, it might be better to divide the slope region into two or more regions, depending on the goal of the research. In addition, defining a region between the building and dune profile could help to interpret the model results, since this section might supply or trap sediment explaining patterns that are found downwind. In addition, the region between the buildings and dune contains significant changes to bed morphology. This region can either form a sediment trap or provide a supply of sediment for the downwind region depending on the building characteristics which could help to understand the patterns that are observed downwind of the buildings, over the dune profile.

Bibliography

[1] P. Pourteimouri, G. H. P. Campmans, K. M. Wijnberg, and S. J. M. H. Hulscher, "Modelling the influence of beach buildings with different pole heights on aeolian morphologic patterns, and their significance for the duneward sediment transport," In prep.

[2] WOTY, "Strandhuisjes nederland; lekker uitwaaien op het strand!" 2022. , doi: https://woty.nl/strandhuisjes-nederland/

[3] P. Pourteimouri, G. H. P. Campmans, K. M. Wijnberg, and S. J. M. H. Hulscher, "A numerical study on the impact of building dimensions on airflow patterns and bed morphology around buildings at the beach," *Journal of Marine Science and Engineering*, vol. 10, no. 1, p. 13, 2021. , doi: doi.org/10.3390/jmse10010013

[4] O. Durán, P. Claudin, and B. Andreotti, "On aeolian transport: Grain-scale interactions, dynamical mechanisms and scaling laws." *Aeolian Research*, vol. 3, no. 3, pp. 243–270, 2011. , doi: 10.1016/j.aeolia.2011.07.006

[5] R. V. Bommel, "Strandhuisjes zuiderstrand aanbesteding: Definitief ontwerp," *Ingenieursbureau Den Haag*, no. 95017491, 2014.

[6] M. Garritsen, "Nieuwbouw strandhuis," *MarjoleinGarritsen*, no. V1, 2014.

[7] R. C. D. Zeeuw and M. A. D. Schipper, "Uav lidar: Meting zandmotor duinontwikkeling," *Shore Monitoring Research B.V.*, 2017.

[8] S. Lucrezi, M. Saayman, and P. V. der Merwe, "An assessment tool for sandy beaches: A case study for integrating beach description, human dimension, and economic factors to identify priority management issues," *Ocean Coastal Management*, vol. 121, pp. 1–22, 2016. , doi: 10.1016/j.ocecoaman.2015.12.003

[9] N. L.Jackson and K. F. Nordstrom, "Aeolian sediment transport and landforms in managed coastal systems: A review," *Aeolian Research*, vol. 3, no. 2, pp. 181–196, 2011. , doi: 10.1016/j.aeolia.2011.03.011

[10] M. E. Hanley, S. P. G. Hoggart, D. J. Simmonds, A. Bichot, M. A. Colangelo, F. Bozzeda, H. Heurtfeux, B. Ondiviela, R. Ostrowski, M. Recio, R. Trude, E. Zawadzka-Kahlau, and R. C. Thompson, "Shifting sands? coastal protection

by sand banks, beaches and dunes," *Coastal Engineering*, vol. 87, pp. 136–146, 2014. , doi: 10.1016/j.coastaleng.2013.10.020

[11] T. Fernández-Montblanc, E. Duo, and P. Ciavola, "Dune reconstruction and revegetation as a potential measure to decrease coastal erosion and flooding under extreme storm conditions," *Ocean and Coastal Management*, vol. 188, no. 105075, 2020. , doi: 10.1016/j.ocecoaman.2019.105075

[12] O. Durán and L. J. Moore, "Vegetation controls on the maximum size of coastal dunes," *Proceedings of the National Academy of Sciences (PNAS)*, vol. 110, no. 43, pp. 17 217–17 222, 2013. , doi: 10.1073/pnas.1307580110

[13] K. Nordstrom and J. M. McCluskey, "The effects of houses and sand fences on the eolian sediment budget at fire island, new york," *Journal of Coastal Research*, vol. 1, no. 1, pp. 39–46, 1985. , doi: 10.1016/j.aeolia.2011.03.011

[14] N. Hobeika, C. García-Sánchez, I. Paden, and S. Vitalis, "Cfd, sensitivity analysis and optimisation to promote the formation of dunes," *TU Delft*, 2021.

[15] D. W. Poppema, "Morphological effects of buildings in a sandy beach environment," *Dissertation of University of Twente*. , doi: 10.3990/1.9789036553520

[16] P. Pourteimouri, G. H. P. Campmans, K. M. Wijnberg, and S. J. M. H. Hulscher, "How wind direction and building spacing influences airflow patterns and sediment transport patterns around a row of beach buildings: A numerical study," *Aeolian Research*, vol. 61, no. 100867, 2023. , doi: doi.org/10.1016/j.aeolia.2023.100867

[17] A. V. Stevers, C. García-Sánchez, G. Agugiaro, I. Paden, and M. P. Esch, "The effects of beach house configurations on dune-ward sediment transport," *TU Delft*, 2021.

[18] A. J. Jonkheer, "Assessment of the influence of incident wind angle and dune slope inclination on sediment transport patterns in coastal dunes," *University of Twente*, 2022.

[19] B. M. Hoonhout and S. D. Vries, "A process-based model for aeolian sediment transport and spatiotemporal varying sediment availability," *Advanced Earth and Space Science*, vol. 121, no. 8, pp. 1555–1575, 2016. , doi: 10.1002/2015JF003692

[20] T. von Kármán, "Turbulence and skin friction," *Journal of the Aeronatuical Sciences*, vol. 1, no. 1, pp. 1–20, 1934. , doi: 10.2514/8.5

[21] I. J. Walker and W. G. Nickling, "Dynamics of secondary airflow and sediment transport over and in the lee of transverse dunes," *Progress in Physical Geography*, vol. 26, no. 1, pp. 47–75, 2002. , doi: 10.1191/0309133302pp325ra

[22] J. F. Kok, E. J. R. Parteli, T. I. Michaels, and D. B. Karam, “The physics of wind-blown sand and dust,” *Progress in Physical Geography*, vol. 75, no. 10, 2012. , doi: 10.1088/0034-4885/75/10/106901

[23] D. J. Sherman, B. Li, J. T. Ellis, E. J. Farrell, L. P. Maia, and H. Granja, “Recalibrating aeolian sand transport models,” *Earth Surface Processes and Landforms*, vol. 38, no. 2, pp. 169–178, 2013. , doi: 10.1002/esp.3310

[24] R. G. D. Davidson-Arnott, K. MacQuarrie, and T. Aagaard, “The effect of wind gusts, moisture content and fetch length on sand transport on a beach,” *Geomorphology*, vol. 68, no. 1-2, pp. 115–129, 2005. , doi: 10.1016/j.geomorph.2004.04.008

[25] P. S. Jackson and J. C. R. Hunt, “Turbulent wind flow over a low hill,” *Quarterly Journal of the Royal Meteorological Society*, vol. 101, no. 430, pp. 929–955, 1975. , doi: 10.1002/qj.49710143015

[26] P. J. Mason and R. I. Sykes, “Flow over an isolated hill of moderate slope,” *Quarterly Journal of the Royal Meteorological Society*, vol. 105, no. 444, pp. 383–395, 1979. , doi: 10.1002/qj.49710544405

[27] T. A. G. Smyth, “A review of computational fluid dynamics (cfd) airflow modelling over aeolian landforms,” *Aeolian Research*, vol. 22, pp. 153–164, 2016. , doi: 10.1016/j.aeolia.2016.07.003

[28] B. E. Launder and D. B. Spalding, “Computer methods in applied mechanics and engineering,” vol. 3, no. 2, pp. 3–51, 1976. , doi: 10.1016/0045-7825(74)90029-2

[29] A. B. Smith, D. W. T. Jackson, J. A. G. Cooper, and L. Hernández-Calvento, “Quantifying the role of urbanization on airflow perturbations and dunefield evolution,” *Earth’s Future*, vol. 5, no. 5, pp. 520–539, 2017. , doi: 10.1002/2016EF000524

[30] H. Tsoar, B. White, and E. Berman, “The effect of slopes on sand transport - numerical modelling,” *Landscape and Urban Planning*, vol. 34, no. 3-4, pp. 171–181, 1996. , doi: 10.1016/0169-2046(95)00235-9

[31] A. G. Smyth and P. A. Hesp, “Aeolian dynamics of beach scraped ridge and dyke structures,” *Coastal Engineering*, vol. 99, pp. 38–45, 2015. , doi: 10.1016/j.coastaleng.2015.02.011

[32] P. A. Hesp and A. G. Smyth, “Jet flow over foredunes,” *Earth Surface Processes and Landforms*, vol. 41, no. 12, pp. 1727–1735, 2016. , doi: 10.1002/esp.3945

[33] ——, “Cfd flow dynamics over model scarps and slopes,” *Physical Geography*, vol. 42, no. 1, pp. 1–24, 2021. , doi: 10.1080/02723646.2019.1706215

[34] G. Qian, Z. Dong, W. Luo, and J. Lu, “Mean airflow patterns upwind of topographic obstacles and their implications for the formation of echo dunes:a wind tunnel simulation of the effects of windward slope,” *Journal of Geophysical Research*, vol. 116, no. F4, 2011. , doi: 10.1029/2011JF002020

[35] G. Qian, Z. Dong, W. Luo, Z. Zhang, and A. Zhao, “Airflow patterns upwind of obstacles and their significance for echo dune formation: A field measurement of the effects of the windward slope angle,” *Science China Earth Sciences*, vol. 55, pp. 545–553, 2012. , doi: 10.1007/s11430-011-4248-4

[36] M. S. Fadl and J. Karadelis, “Cfd simulation for wind comfort and safety in urban area: A case study of coventry university central campus,” *International Journal of Architecture, Engineering and Construction*, vol. 2, no. 2, pp. 131–143, 2013. , doi: 10.7492/IJAEC.2013.013

[37] P. Pourteimouri, “The impact of buildings at beaches on airflow and aeolian sediment transport patterns across beach-dune topography, using cfd modelling: Literature report,” *University of Twente: Faculty of Engineering Technology*, p. 67, 2020. , doi: 10.7492/IJAEC.2013.013

[38] R. A. Bagnold, “The transport of sand by wind,” *The Geographical Journal*, vol. 89, no. 5, pp. 409–438, 1937.

[39] ——, “The physics of blown sand and desert dunes. methuen, london.” p. 265, 1941.

[40] R. Kawamura, “Study on sand movement by wind,” *Reports of Physical Sciences Research Institute of Tokyo University*, vol. 5, no. 3-4, pp. 95–112, 1951.

[41] A. W. Zingg, “Wind tunnel studies of the movement of sedimentary matrial,” *Proceedings of the 5th Hydraulic Conference Bulletin*, vol. 34, pp. 111–135, 1953.

[42] P. R. Owen, “Saltation of uniform grains in air,” *Journal of Fluid Mechanics*, vol. 20, pp. 225–242, 1964.

[43] S.-A. Hsu, “Computing eolian sand transport from shear velocity measurements,” *Journal of Geology*, vol. 81, pp. 739–743, 1973.

[44] K. Lettau and H. H. Lettau, “Experimental and micrometeorological field studies of dune migration,” *Exploring the World’s Driest Climate*, pp. 110–147, 1978.

[45] L. C. V. Rijn and G. Strypsteen, “A fully predictive model for aeolian sand transport,” *Coastal Engineering*, vol. 156, no. 103600, 2020. , doi: 10.1016/j.coastaleng.2019.103600

[46] S. D. Vries, J. S. M. V. T. de Vries, L. C. V. Rijn, S. M. Arens, and R. Ranasinghe, “Aeolian sediment transport in supply limited situations,” *Aeolian Research*, vol. 12, pp. 75–85, 2014. , doi: 10.1016/j.aeolia.2013.11.005

[47] S. D. Vries, H. N. Southgate, W. Kanning, and R. Ranasinghe, “Dune behavior and aeolian transport on decadal timescales,” *Coastal Engineering*, vol. 67, pp. 41–53, 2012. , doi: 10.1016/j.coastaleng.2012.04.002

[48] C. R. Sloss, M. Shepherd, and P. A. Hesp, “Vegetation controls on the maximum size of coastal dunes,” *Nature Education Knowledge*, vol. 3, no. 10, p. 2, 2012.

[49] P. A. Hesp, R. Davidson-Arnott, I. J. Walker, and J. Ollerhead, “Flow dynamics over a foredune at prince edward island, canada,” *Geomorphology*, vol. 65, pp. 71–84, 2005. , doi: 10.1016/j.geomorph.2004.08.001

[50] J. G. S. Keijsers, A. V. D. Groot, and M. J. P. M. Riksen, “Vegetation and sedimentation on coastal foredunes,” *Geomorphology*, vol. 228, pp. 723–734, 2015. , doi: 10.1016/j.geomorph.2014.10.027

[51] K. F. Nordstrom, R. Lampe, and L. M. Vandemark, “Reestablishing naturally functioning dunes on developed coasts,” *Environmental Management*, vol. 25, pp. 37–51, 2000. , doi: 10.1007/s002679910004

[52] C. Paola and V. R. Voller, “A generalized exner equation for sediment mass balance,” *Journal of Geophysical Research: Earth Surface*, vol. 110, no. F4, 2005. , doi: 10.1029/2004JF000274

[53] S. Leliavsky, *An Introduction to Fluvial Hydraulics*, 1955.

[54] S. V. Meijeren and R. W. Vaessen, “Passende beoordeling strandhuisjes kijkduin,” *Dactylis V.O.F.*, no. 14005, 2014.

[55] Windfinder, “Wind statistics at kijkduin based on observations over the period 10/2014 - 10/2018,” 2023. , doi: https://www.windfinder.com/forecast/kijkduin_den_haag

[56] B. Hoonhout, “In aeolis sourcecode included comments,” *Deltares: Unit of Hydraulic Engineering*, 2015.

[57] T. J. Glover, “Pocket pc reference,” *Sequoia Pub, 2nd edition (Cited by Beakawi Al-Hashemi and Baghabra Al-Amoudi, 2018)*, 1996.

[58] B. Hoonhout and J. V. T. D. Vries, “Invloed van strandbebouwing op zandverstuiving: Adviezen voor vergunningverleners,” *Deltares*, no. 1207724-000, 2013.

[59] M. Jansen, “Personal communication with s. van meijeren and r. w. vaessen,” *Witteveen+Bos*, 2014.

[60] R. K.-D. Heijer, “Effect strandhuisbebouwing op verstuiving (presentation),” *Deltares*, 2014.

[61] N. Smit and R. C. D. Zeeuw, “Uav lidar: Meting zandmotor duinontwikkeling,” *Shore Monitoring Research B.V.*, 2018.

[62] W. Luo, Z. Dong, G. Qian, and J. Lu, “Near-wake flow patterns in the lee of adjacent obstacles and their implications for the formation of sand drifts: A wind tunnel simulation of the effects of gap spacing,” *Geomorphology*, vol. 213, pp. 190–200, 2014. , doi: 10.1016/j.geomorph.2014.01.008

[63] S. M. Arens, J. P. M. Mulder, Q. L. Slings, L. H. W. T. Geelen, and P. Damsma, “Dynamic dune management, integrating objectives of nature development and coastal safety: Examples from the netherlands,” *Geomorphology*, vol. 199, pp. 205–213, 2013. , doi: 10.1016/j.geomorph.2012.10.034

[64] B. Hoonhout and S. D. Vries, “Field measurements on spatial variations in aeolian sediment availability at the sand motor mega nourishment,” *Aeolian Research*, vol. 24, pp. 93–104, 2017. , doi: 10.1016/j.aeolia.2016.12.003

[65] B. O. Bauer, R. G. D. Davidson-Arnott, P. A. Hesp, S. L. Namikas, J. Ollerhead, and I. J. Walker, “Aeolian sediment transport on a beach: Surface moisture, wind fetch, and mean transport,” *Geomorphology*, vol. 105, pp. 106–116, 2009. , doi: 10.1016/j.geomorph.2008.02.016

A. Sedimentation patterns in x-y plane

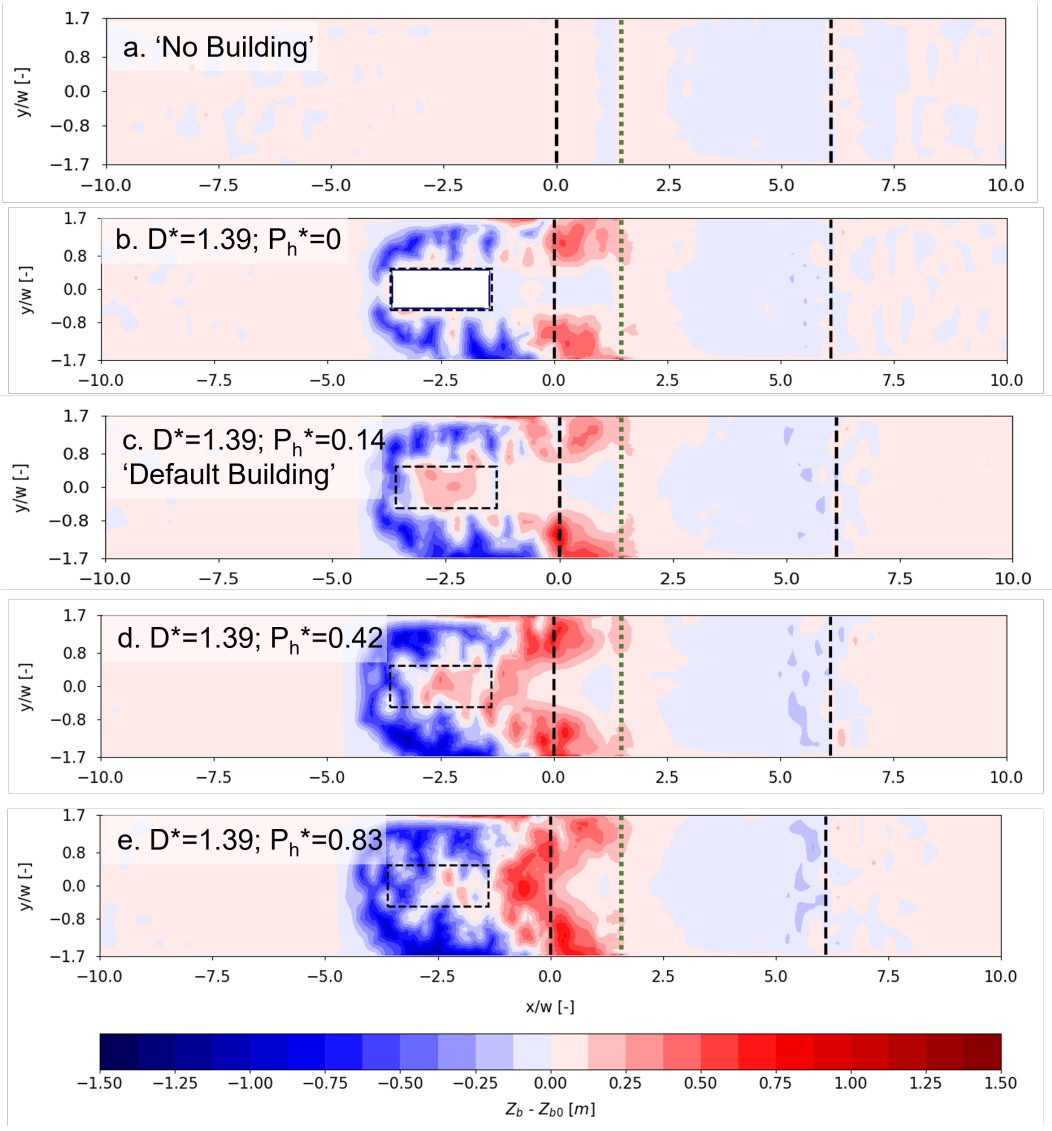

Figure 28: Sedimentation patterns (Z_b - Z_{b0}) over 24 hours for the configurations without buildings (a. 'No Building') and with the following distance ratio and pole height ratio: 1.39; 0 (b.), 1.39; 0.14 (c.), 1.39; 0.42 (d.) and 1.39; 0.83 (e.). The dune toe and top are indicated by a black dashed bar over the width of the domain. A green dashed line indicates the cross-shore starting location of the vegetation.

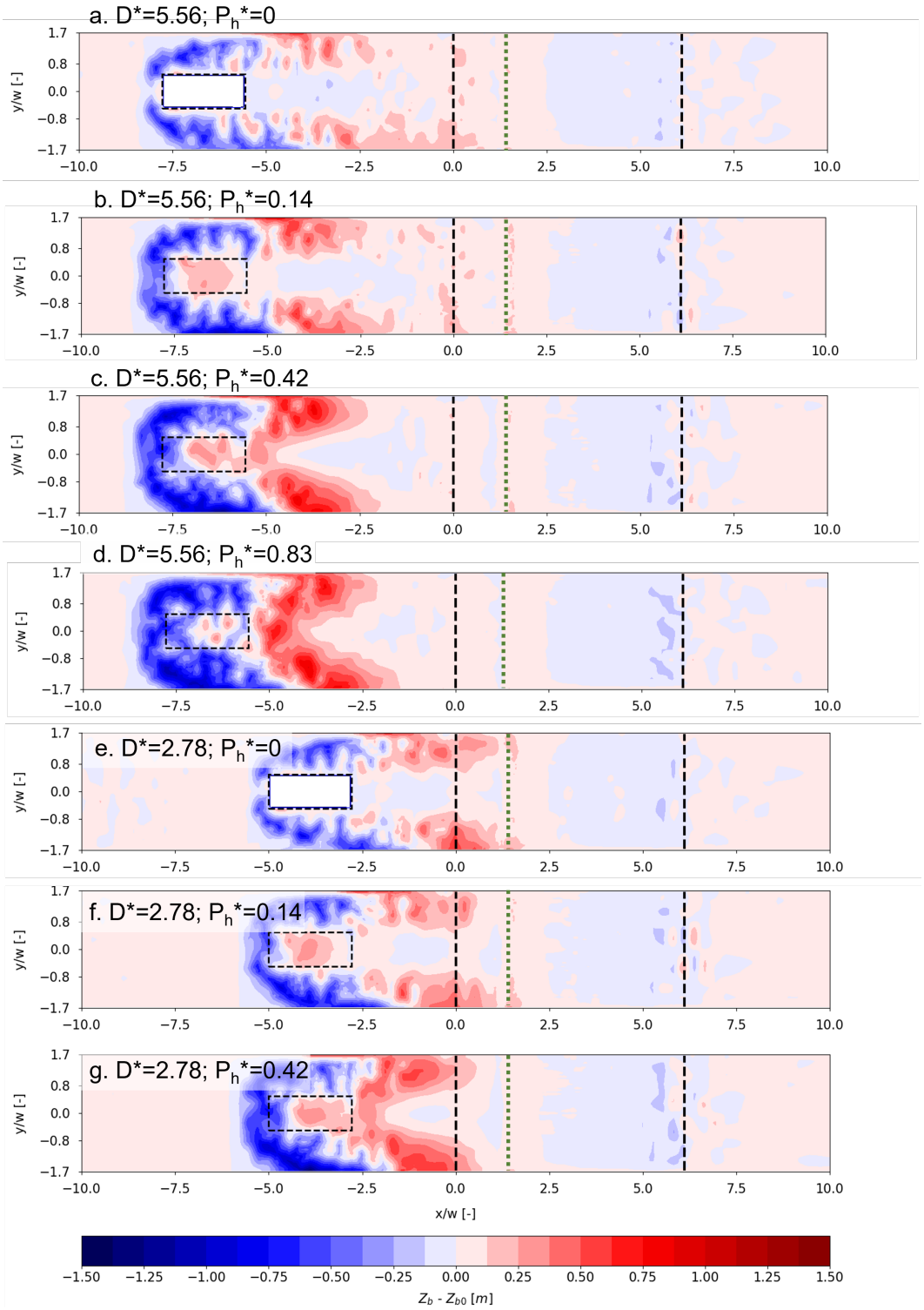

Figure 29: Sedimentation patterns (Z_b - Z_{b0}) over 24 hours for the configurations with the following distance ratio and pole height ratio: 5.56; 0 (a.), 5.56; 0.14 (b.), 5.56; 0.42 (c.) and 5.56; 0.83 (d.) 2.78; 0 (e.), 2.78; 0.14 (f.) and 2.78; 0.42 (g.). The dune toe and top are indicated by a black dashed bar over the width of the domain. A green dashed line indicates the cross-shore starting location of the vegetation.

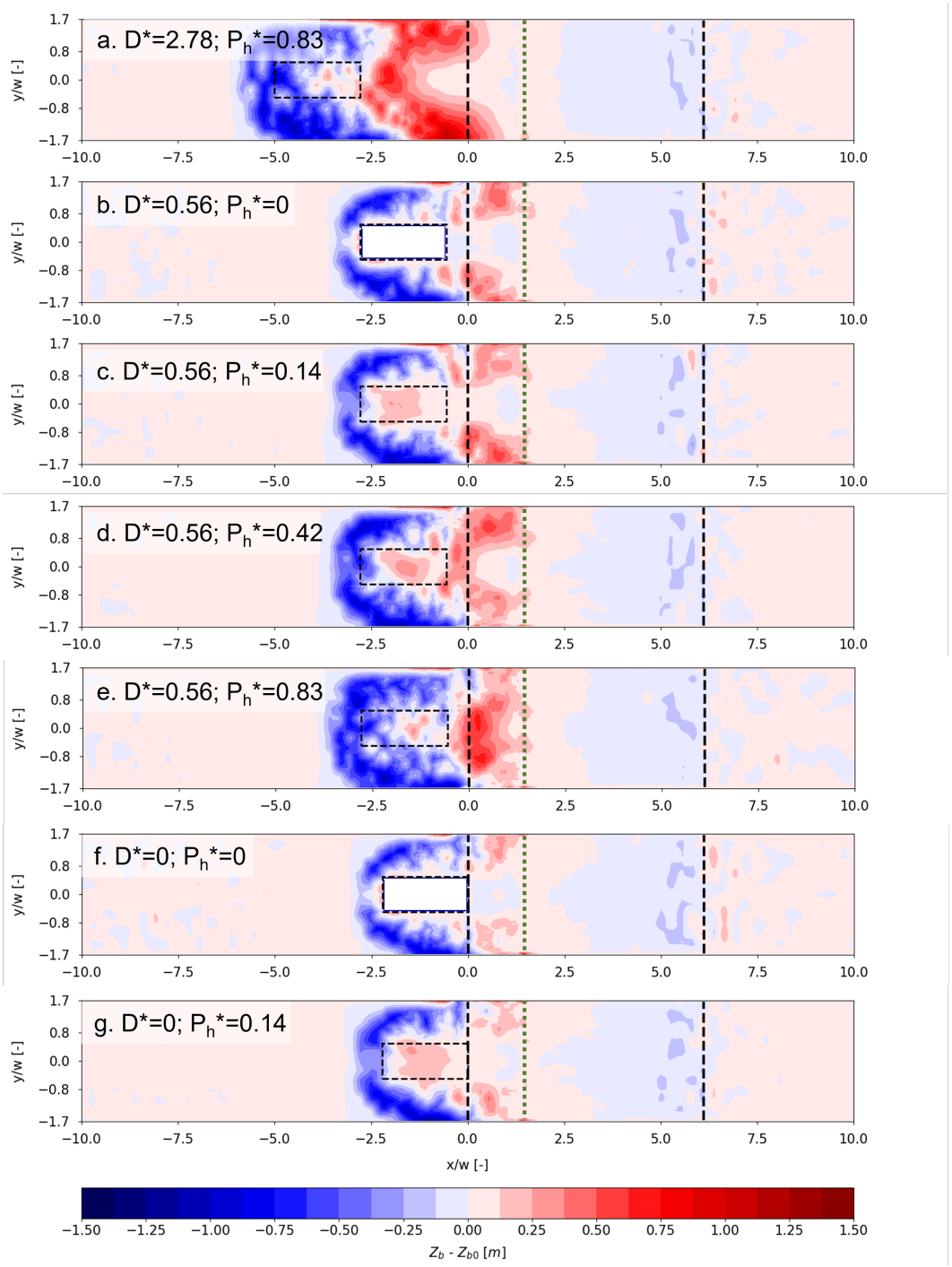

Figure 30: Sedimentation patterns (Z_b - Z_{b0}) over 24 hours for the configurations with the following distance ratio and pole height ratio: 2.78; 0.83 (a.), 0.56; 0 (b.), 0.56; 0.14 (c.) and 0.56; 0.42 (d.) 0.56; 0.83 (e.), 0; 0 (f.) and 0; 0.14 (g.). The dune toe and top are indicated by a black dashed bar over the width of the domain. A green dashed line indicates the cross-shore starting location of the vegetation.

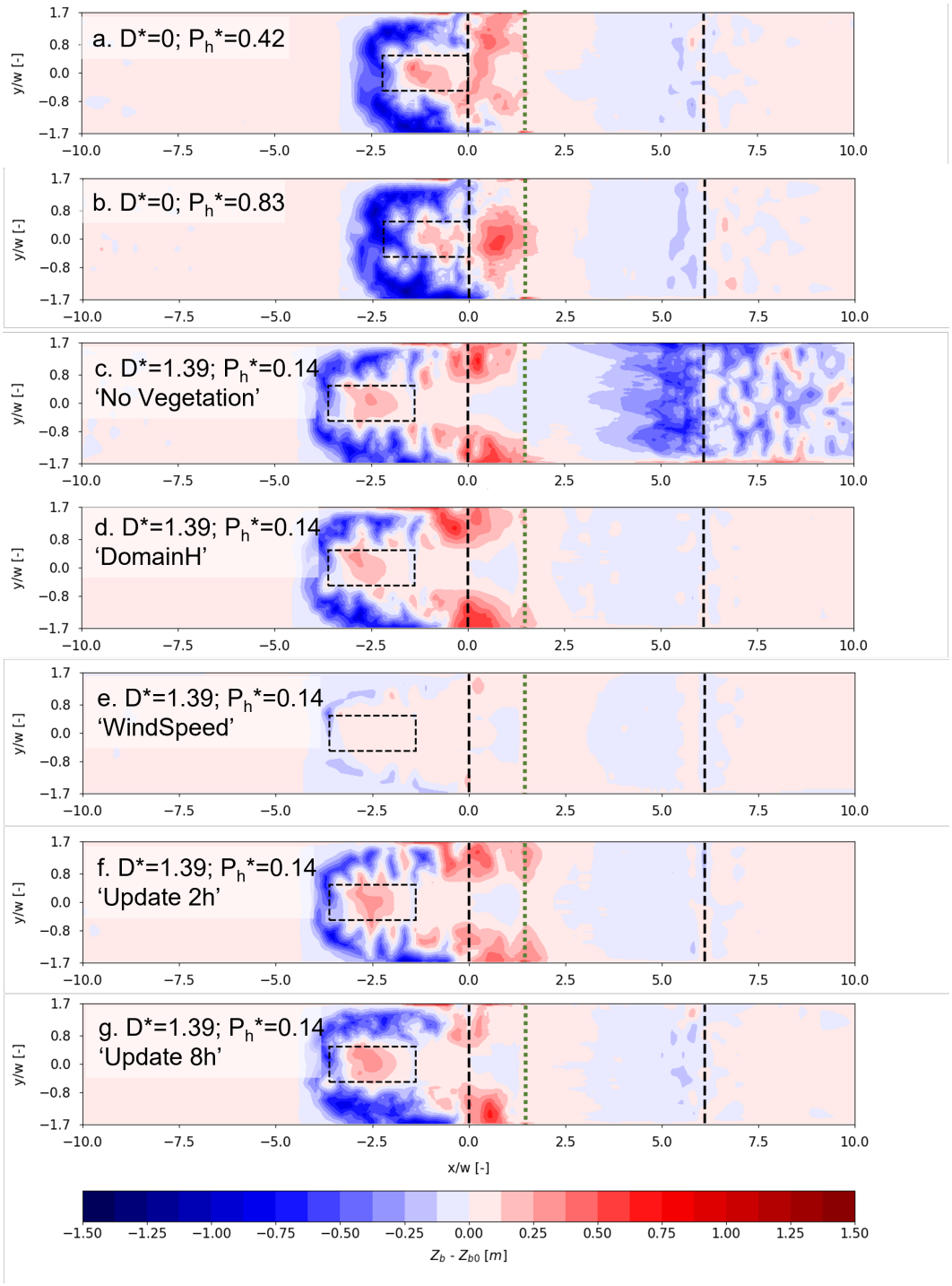

Figure 31: Sedimentation patterns (Z_b - Z_{b0}) over 24 hours for the configurations with the following distance ratio and pole height ratio: 0; 0.42 (a.) and 0; 0.83 (b.). Additionally, configurations without vegetation (c.), domain height of 80 meters (d.), wind speed of 10 m/s (e.) and time step between two wind field updates of 2 hours (f.) and 8 hours (g.) are shown for distance ratio 1.39 [-] and pole height ratio 0.14 [-]. The dune toe and top are indicated by a black dashed bar over the width of the domain. A green dashed line indicates the cross-shore starting location of the vegetation.

B. Model parameter settings

In this chapter, the settings for OpenFOAM and AeoLiS are presented for the reproducibility of this study. The coupling model requires approximately 5 hours to compute 24 hours of aeolian sediment transport with 6 updates of the wind field at equal time intervals based on morphological bed evolution. The computation time is based on the usage of the computational cluster of Witteveen+Bos with a clock speed of 2.20 GHz. The OpenFOAM model uses 16 cores which takes approximately 40 minutes per wind field computation. AeoLiS runs on 1 core and takes approximately 2 minutes. Thus, in comparison to the OpenFOAM model, AeoLiS is significantly less computationally expensive. Additional Python files prepare the required files as input for OpenFOAM and AeoLiS and take approximately 8 minutes per iteration round on 1 core.

B.1 OpenFOAM settings

In OpenFOAM, the model settings are mainly included in the 'fvsolution' file. This file defines the solvers that are used and stop the computation if residuals fall below a threshold value. The settings as defined in the 'fvsolution' file are provided in table B.1. In addition, one computation of the wind field through OpenFOAM usually converges after approximately 180 iterations.

B.2 AeoLiS Settings

In AeoLiS, the settings are defined in 'Main_Input_File.txt'. The parameter settings in this file can be found on the next page.

Table B.1: OpenFOAM settings in fvsolution for p, U, k and ϵ

Parameter	Solver	Smoother	Tol	RelTol	ResCont	RelaxFac
p	GAMG	GaussSeidel	1e-06	0.001	1e-02	0.9
U	smoothSolver	symGaussSeidel	1e-08	0.001	1e-03	0.9
k	smoothSolver	symGaussSeidel	1e-08	0.001	1e-03	0.9
ϵ	smoothSolver	symGaussSeidel	1e-08	0.001	1e-03	0.9

```
                Aa = 0.085
               CFL = 1
                Cb = 1.5
               Cdk = 5
                Ck = 2.78
                Cl = 6.7
                 L = 100
                 T = 1
              Tdry = 5400
             Tsalt = 2592000
            Tswash = 30
             V_lat = 0
             V_ver = 0
              alfa = 0
       beach_slope = 0
          bed_file = Z_Grid_Round_Counter.txt
              beta = 130
                bi = 1
 boundary_lateral = circular
boundary_offshore = constant
 boundary_onshore = constant
               c_b = 0.2
constant_offshore_flux = 0
 constant_onshore_flux = 0
             cpair = 0.0010035
             csalt = 0.035
                dt = 60
dune_toe_elevation = 0
                dx = 1
                dy = 1
      dzb_interval = 86400
           dzb_opt = 0
               eps = 0.001
            facDOD = 0.1
      fence_file = fence.grd
                 g = 9.81
             gamma = 0.5
   gamma_vegshear = 16
        germinate = 0
   grain_dist = 1
   grain_size = 0.0003
         hveg_max = 1
                 k = 0.001
             kappa = 0.41
                 l = 10
          lateral = 0
    lateral_flux = 0
  layer_thickness = 0.005
                 m = 0.5
        max_error = 0.000001
         max_iter = 1000
    method_moist = belly_johnson
 method_transport = bagnold
             mu_b = 30
       nfractions = 1
          nlayers = 1
               nx = Number_of_cells_X
               ny = Number_of_cells_Y
    offshore_flux = 0
    okin_c1_fence = 0.48
      okin_c1_veg = 0.48
okin_initialred_fence = 0.32
  okin_initialred_veg = 0.32
    onshore_flux = 0
    output_times = 3600
     output_file = Output_File.nc
     output_vars = zb zs zsep ustar0 ustar ustarn ustars uth uth0 u us un Ct Cu w mass pickup tau q qs qn
         ne_file = Non_Erodible_Layer_Information.txt
        porosity = 0.4
process_avalanche = T
process_bedupdate = T
 process_dune_erosion = F
      process_fences = F
 process_humidity = F
  process_inertia = F
    process_meteo = F
```

```
 process_mixtoplayer = F
       process_moist = F
     process_nelayer = T
       process_runup = F
        process_salt = F
  process_separation = F
       process_shear = T
   process_threshold = T
        process_tide = F
   process_transport = T
  process_vegetation = T
        process_wave = F
process_wave_coupled = F
        process_wind = T
       process_swash = F
  process_lagoon = F
     tide_lagoon = 0
     wave_lagoon = 0
    start_lagoon = 0
 process_lagoonswash = F
                rhoa = 1.293
                rhog = 2650
                rhow = 1025
              scheme = euler_backward
       sedimentinput = 0
               sigma = 4.20
              solver = pieter
         th_bedslope = F
         th_drylayer = F
        th_grainsize = T
         th_humidity = F
         th_moisture = F
          th_nelayer = F
        th_roughness = T
             th_salt = F
          theta_dyn = 33
          theta_stat = 34
          tide_file = Tide_Information.txt
             tstart = 0
              tstop = 14400
                  v = 0.000014
           veg_file = Vegetation_Information.txt
          veg_gamma = 1
   veg_min_elevation = 3
          veg_sigma = 0.8
       vegshear_type = raupach
          wave_file = wave.txt
     wind_convention = nautical
          wind_file = Wind_Information.txt
         xgrid_file = X_Grid.txt
                 xi = 0.3
         ygrid_file = Y_Grid.txt
                  z = 10
wallShearStress_file = Modified_wallShearStress_Round_Counter.txt
```

C. Model lateral boundary correction

As mentioned in chapter 3.1.3, OpenFOAM requires equal lateral side patches for the use 'CyclicAMI' cyclic boundary condition. Therefore, the bed at the lateral sides of the domain is required to be equal in elevation, which has been found to contain small inconsistencies. To deal with unequal sides, a correction is performed over the elevation value of the lateral side grid points in AeoLiS. Prior to the correction, the boundary points at both ends (black) of the grid are assigned the same value, which corresponds to the average elevation of the adjacent grid points (light green) into the domain. Since this may lead to rather extreme corrections at the sides, the adjacent grid points (light green) are corrected in a similar way with the adjacent grid points (light red), see figure 33.

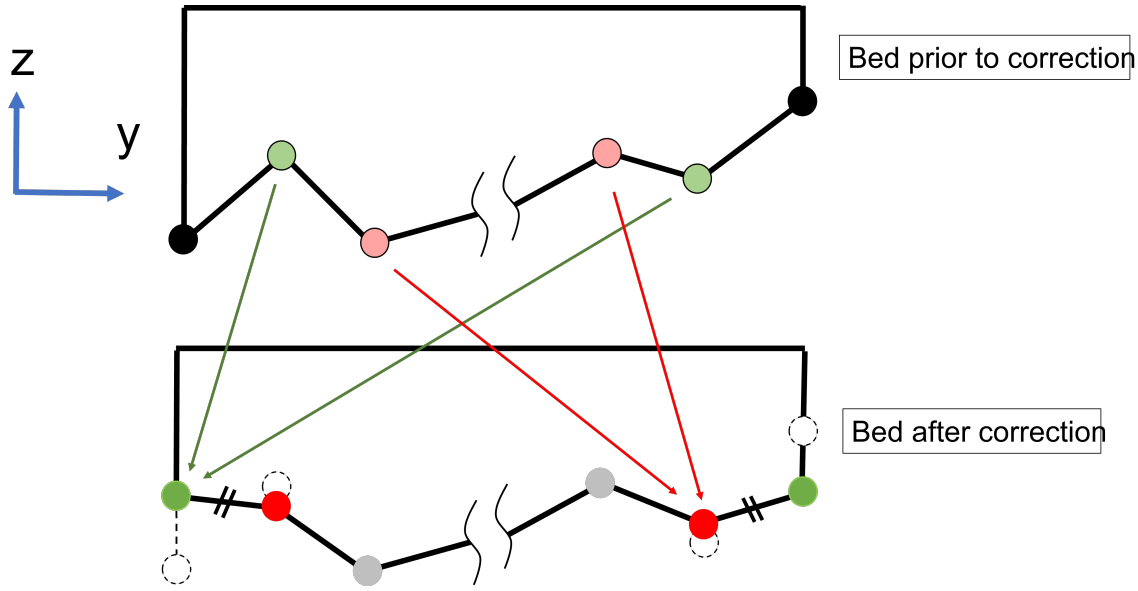

Figure 32: In the figure it can be seen how the bed is corrected after an AeoLiS simulation is completed to prepare the bed on the lateral sides of the domain for computation of the wind field in OpenFOAM. The top figure shows the bed before the correction and the bottom figure shows the bed after the correction is performed. The correction ensures that the two most outer grid points at both lateral sides share equal bed level elevation.

D. Model implementation dune shape

The dune shape that has been used in this research has been created similarly as Jonkheer et al. [18]. A schematized overview is provided in figure 33. The cross-shore length of the curvature at the dune toe and dune crest is defined as $\frac{1}{5}$th of the cross-shore inclined dune length (in figure 5). In between the curvatures, a straight line is drawn with slope θ_{dune}, which is 30°. The curvature is smooth to have a continuous slope derivative over the entire dune profile. The shape of the dune is defined in cross-shore direction with increments of 0.2 m to allow for the smoothening of the curvatures.

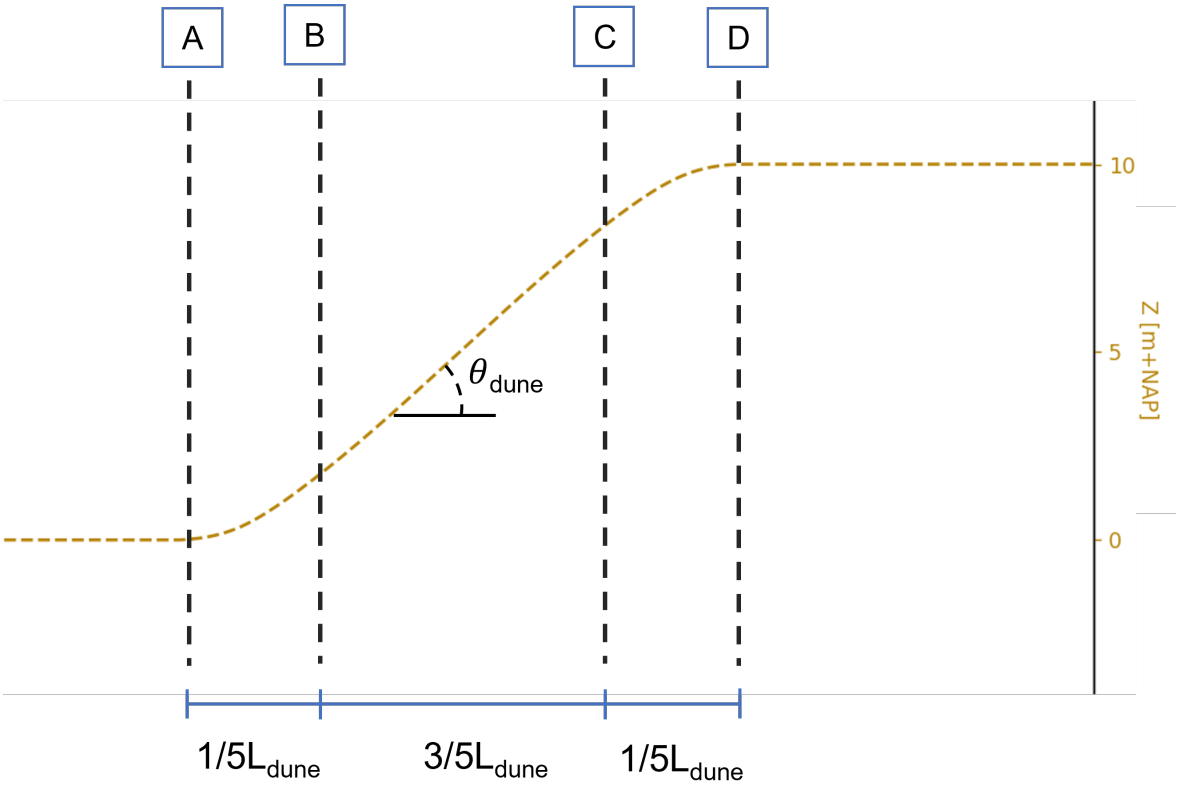

Figure 33: A schematized overview of the definition of the dune profile. L_{dune} represents the total cross-shore length of the inclined section of the dune profile from the dune toe (0 m+NAP) up to the dune crest (10 m+NAP).

E. Inlet and outlet boundary condition

The inlet and outlet boundaries have been chosen to minimize effects on modeling results. Both boundaries are defined as zero gradient. Figure 34 shows an overview of the entire cross-domain width. It can be seen that the inlet and outlet do show some divergent bed-level behaviour. At the inlet, this is related to strong erosion due to zero sediment concentration at the inlet. As a result, sediment is entrained up until an equilibrium is formed. At the outlet, it can be seen that the bed level drops significantly at the boundary whereas deposition occurs just upwind of the boundary. However, it should be noted that these boundary effects occur at a substantial distance from the relevant section, within the range of x/w [-10:10].

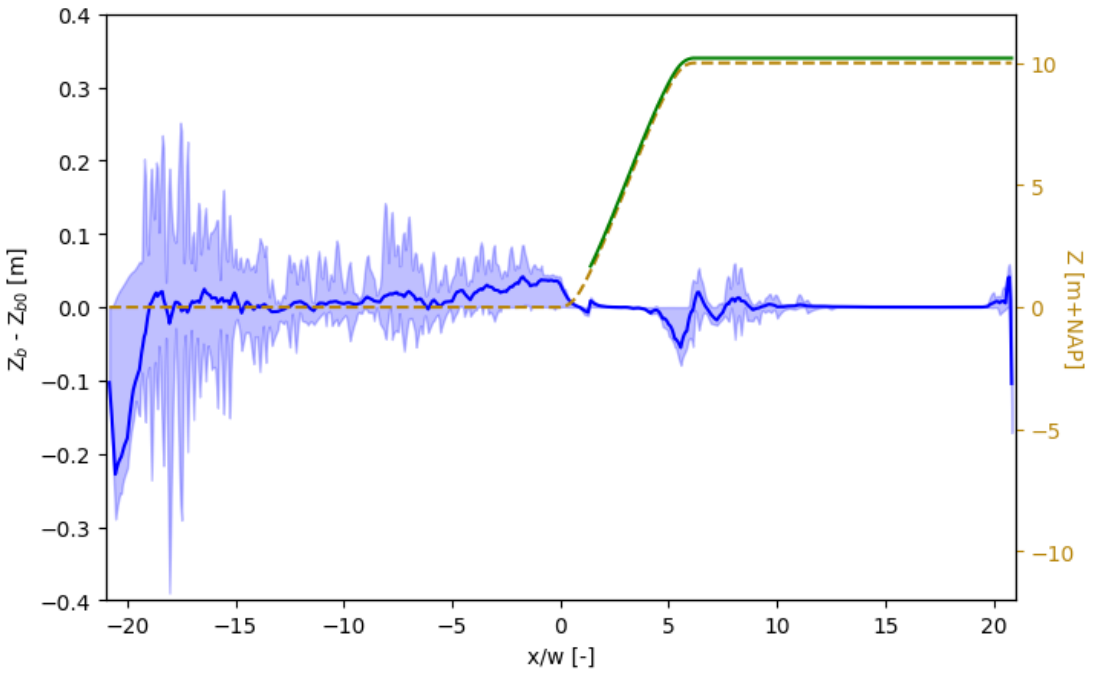

Figure 34: An overview of mean (dark blue), minimum and maximum bed level (light blue) change for the 'No Building' configuration over the entire domain length over 24 hours. The yellow line represents the dune profile and the green line the location of the vegetation.